ABSTRACT

Title of Thesis:	POLYCYCLIC AROMATIC HYDROCARBONS (PAHS) AND PAH DEGRADING BACTERIA IN MEDIA OF A STORMWATER BIORETENTION CELL
	Chen Yuan, Master of Science, 2020
Thesis Directed By:	Assistant Professor, Birthe Kjellerup, Civil and Environmental Engineering

Polycyclic aromatic hydrocarbons (PAHs) are a group of organic pollutions that are carcinogenic to humans. A bioretention cell at the campus of University of Maryland, College Park, evaluated for their potential to remove PAHs from stormwater. The risk of PAH pollution was confirmed by the fact that the highest value of total PAH concentration (25.5 μg/g) and the average concentrations of pyrene (1.78 μg/g) and chrysene (1.40 μg/g) was higher than their respective probable effect concentrations (PECs) (22.8 μg/g, 1.52 μg/g and 1.29 μg/g),. Sources of PAHs in the media originated from fossil fuel combustion and petroleum. Human carcinogenicity was evaluated by determining the Benzo[a]pyrene Total Toxicity Equivalent (BaP-TEQ), and benzo[a]pyrene made most contribution to carcinogenicity. Biotransformation of PAH is possible in bioretention cell, because PAH-ring cleaving dioxygenases (PAH-RCD) gene was found in media.

POLYCYCLIC AROMATIC HYDROCARBONS (PAHS) AND PAH DEGRADING BACTERIA IN MEDIA OF A STORMWATER BIORETENTION CELL

by

Chen Yuan

Thesis submitted to the Faculty of the Graduate School of the
University of Maryland, College Park, in partial fulfillment
of the requirements for the degree of
Master of Science
2020

Advisory Committee:
Dr. Birthe Kjellerup, Chair
Dr. Allen Davis
Dr. Alba Torrents

Table of Contents

Chapter 1

Polycyclic Aromatic Hydrocarbons (PAHs) and PAH Degrading Bacteria in Media of a Stormwater Bioretention Cell

Chen Yuan, Allen P. Davis, Devrim Kaya and Birthe V. Kjellerup

Department of Civil and Environmental Engineering, University of Maryland College Park

Abstract

This research investigated the distribution of 16 EPA priority PAHs and their toxicity in the bioretention cell. The Highest total PAH concentration found in the media was 25.48 μg/g, and individual PAHs with highest average concentrations were banzo[g,h,i]perylene in February and pyrene in June. The PAH concentrations in surface samples did not show a clear trend. Sources of PAHs were fossil fuel combustion and petroleum. Ecological impact and carcinogenicity to humans of bioretention cell media were assessed by probable effect concentrations (PECs) and benzo[a]pyrene total toxicity equivalent (BaP-TEQ) respectively. The results show that average concentrations of pyrene and chrysene exceed PECs, and the average BaP-TEQ was 1.64 μg/g, which mainly contributed by benzo[a]pyrene. Results of PCR showed that there was one kind of PAH-ring cleaving dioxygenases (PAH-RCD) gene (C12O) in the media, which means that the aerobic biodegradation of PAHs is possible in the bioretention cell.

1. Introduction

Polycyclic aromatic hydrocarbons (PAHs) are a group of organic compounds that consist of two or more aromatic rings in the form of a fused ring compound. More than 100 compounds exist within the group of PAHs from naphthalene (molecular weight of 128 g/mol, log K_{ow} of 3.32) to coronene (molecular weight of 300 g/mol, log K_{ow} of 6.75) (Lu et al., 2008; Pyrene and Analogues, 1983). PAHs are present in many compartments of the environment due to their resistance to biodegradation (Crampon et al., 2014) and thus bioaccumulate in the food web (Ribeiro et al., 2005). They are recognized as carcinogenic compounds and some are classified as the human carcinogens (class 1) as categorized by the International Agency for Research on Cancer (IARC, 2012). As a result, PAHs are of significant environmental concern and the U.S. EPA has established regulations for the concentration of PAHs in the environment (Haritash and Kaushik, 2009). The U.S. EPA has issued a list of 16 PAHs that frequently occurred in environment and are known to be toxic (Table 1).

Two known pathways for PAH toxicity are 1) Non-metabolic toxicity and 2) metabolic toxicity (Sikkema et al., 1994). The toxicity of PAHs is mainly attributed to metabolic toxicity (Gauthier et al., 2014). One manifestation of non-metabolic toxicity is membrane damage, which is due to the lipophilicity of PAHs. The distribution of PAHs in the cell membrane causes the membrane to expand and increase fluidity. (Sikkema et al., 1994). Non-metabolic toxicity is also reflected in the fact that PAHs inhibits P-ATPase

(Li et al., 2011). These two effects cause loss of cellular function and cause cell death under continuous influence. Through bioactivation, PAHs will enable metabolic toxicity that leads to carcinogenicity (Gauthier et al., 2014). As an example, Benzo[a]pyrene (BaP) can be epoxygenated to 7,8-dihydrodiol-9,10 epoxide (BPDE). However, it can also form radical cations through 1-electron oxidations. Once formed, those products may bind to nucleophilic sites on DNA and form DNA adducts (Siddens et al., 2012). Based on experiments on animals, BaP was determined to be the most potent carcinogenic PAHs (Haritash and Kaushik, 2009; Kim et al., 2013).

PAHs originate from a wide range of sources such as incomplete combustion of organic materials (fossil fuels and wood) and during industrial processes (Kim et al., 2013). PAHs are also produced by natural processes, such as volcanic eruptions, forest fires and oil seeps (Yunker et al., 2002). Many processes contribute to the accumulation of PAHs in urban landscapes, such as leakage of oil, and abrasion of road surface and tires (El-Mufleh et al., 2013). In addition, PAHs discharged to the atmosphere can be accumulated on ground surfaces by dry and wet deposition. (Esen et al., 2008). Pollutants settled by dry deposition will remain on the surface of ground until they are washed away by rainfall/stormwater (Al Ali et al., 2017). PAHs can also contaminate stormwater directly by wet deposition in the form of rain and snow (Göbel et al., 2006). PAHs consisting of < four rings are mainly removed from the atmosphere by wet deposition since these PAHs tend to present in the gaseous state because of the relatively low log

K_{OA} (Parnis et al., 2015). Dry deposition often takes place for PAHs > four rings, which are mainly distributed on particles due to adsorption (Cheng et al., 2018). Log Kow values of PAHs also increasing with molecular weights (Table 1), which suggests that HMW-PAHs are more likely to be adsorbed on particles in stormwater and adsorbed on media particles after storm water flow into bioretention cell, while LMW-PAHs are relatively easy to transport with stormwater. Partition of PAHs between dissolved and particulate phases was reported by Zgheib (2011), results showed that almost all PAHs, especially HMW-PAHs, are distributed in the particle phase.

PAHs can be transported by particulate matter in stormwater, and if left untreated, they will flow into aquatic ecosystems such as rivers and cause pollution (Estebe, 1997). As a result, stormwater runoff is recognized by the U.S. Environmental Protection Agency (USEPA) as one of the important sources of water quality deterioration (USEPA, 2017). Water quality deterioration can be caused by stormwater from parking lots and streets (Dietz and Clausen, 2006). Urban runoff has caused deterioration of lake water quality and increased concentrations of PAHs (highest concentration: 3.66 μg/g) in sediments (Jung et al., 2008). Howitt (2014) found that PAHs (3.02 to 23.13 μg/g) accumulated in sediments of semi-natural wetland in Victoria, Australia because of stormwater inputs. A variety of PAHs were identified with concentrations ranging from 64 μg/kg to 26288 μg/kg in the sediments of stormwater retention ponds that treat stormwater from golf courses, low and high density residential development, and

commercial development, in the coastal areas of South Carolina, USA (Weinstein et al., 2010). The concentration depended on the land use, with the highest levels (10,422 ± 3944 μg/kg) detected in commercial development.

Bioretention is one of the most efficient and cost effective stormwater control measures (SCMs) (Li and Davis, 2008). This treatment takes advantage of the porous soil media, which consists of soil, sand, and organic matter; stormwater flows through the medium to reduce the concentration of pollutants (Li and Davis, 2008, Jones and Davis, 2013). Several studies have reported the effectiveness of bioretention in the removal of phosphorus, nitrogen, heavy metals, organic pollutants, such as PAHs, PCBs and oil, and pathogens in stormwater (LaBarre et al., 2016, Hong et al., 2006, Wan et al., 2017, Lau et al., 2017, Brown and Hunt 2012, DeBusk et al., 2011). In a study of a bioretention system in the semiarid Daly City, California, USA, PAH concentrations in the stormwater were reduced by 90% (from 2300 to 235 ng/L) with the installation of a bioretention system (David et al., 2014). Diblasi (2008) reported that bioretention cells could reduce 31 to 99% of the PAH event mean concentration and 86% of the PAH mass load; the reduction of PAH concentration was associated with the removal of total suspended solids (TSS).

In addition to physical removal of PAHs via suspended solids removal, microorganisms can enhance the removal of PAHs by degrading the organic compounds (Hong et al., 2006; LeFevre et al., 2011). PAHs are biodegradable in both aerobic and anaerobic environments (Nzila, 2018; Wongwongsee et al., 2013), where various

enzymes play a key role in the involved pathways.

There are three pathways involved in aerobic PAH degradation (Figure 1). These involve cytochrome P-450 monooxygenase, ligninolytic enzymes and PAH ring-hydroxylating dioxygenase (PAH-RHD). Both bacteria and fungi can degrade PAHs through the cytochrome P-450 monooxygenase pathway (Haritash and Kaushik, 2009). Ligninolytic enzymes, such as lignin peroxidases, manganese peroxidases, and laccases, provide PAHs degrading pathways for fungi, while bacteria can also degrade PAHs via the PAH-RHD pathway (Haritash and Kaushik, 2009; Kadri et al., 2017; Syed et al., 2010). Low-molecular-weight PAHs (LMW-PAH), which are PAHs with two and three rings, are generally biodegradable in anaerobic environments. However, anaerobic biodegradation of high-molecular-weight PAHs (HMW-PAH) (> 4 rings) were studied in an anaerobic batch reactor (Nzila, 2018). Examples of bacteria and fungi that can degrade PAHs are shown in Table 2.

Current studies of PAH fate in bioretention cells has not provided sufficient information regarding the presence or distribution of PAHs and PAHs degrading bacteria, and few studies have evaluated the environmental impact of bioretention cell media by PAH concentrations and toxicity. To assess the environmental impact, information about PAH concentrations and spatial distribution is necessary. To evaluate the biodegradation potential of bioretention cells for PAHs, potential PAHs degrading bacteria need to be identified. The overall objectives of this study were (1) to investigate the spatial

distribution of PAHs in a bioretention cell, (2) to identify the sources of PAHs on the campus of University of Maryland based on diagnostic ratios, (3) to estimate toxicity of captured PAHs by calculating the benzo[a]pyrene toxic equivalent quantity (BaP-TEQ) and (4) evaluate if biodegradation of PAHs can occur at the site.

To advance the understanding of the PAH presence and biodegradation in bioretention, surface samples as well as core samples were collected two times during a year at a UMD bioretention cell. These samples were analyzed for PAH concentrations of the 16 EPA required PAHs. The microbial composition of the bioretention surface and core samples were analyzed using molecular tools to determine if biodegradation of PAHs could potentially be occurring in the system.

2. Materials and Methods

2.1 Sampling sites

A bioretention cell that was built in spring 2004 and located at the University of Maryland Campus in College Park MD was investigated. Asphalt parking lots and roads, as well as concrete walkways, form the drainage area with the impervious surface accounting for approximately 90% of the total area. The cell is 50.3 m long and 2.4-4.8m wide with a total area of 181 m^2. A drainage area of approximately 0.28 ha is managed by the bioretention cell (DiBlasi et al., 2009). Four media sampling points were utilized in the bioretention cell, which were located at 0, 0.91, 1.83, and 2.74 m from the inlet of the

cell (Figure 2).

A control sampling point was included in the study. This was located across from the bioretention inlet but was not contacted by stormwater at any time. Core samples of the bioretention media were collected at the depth of 0 to 30 cm, and at sampling points at 0.91, 1.83, and 2.74 m using a Hoffer Soil Sampler (JBK Manufacturing, Dayton, U.S.). The core samples were divided into three segments each 10 cm in length, representing media at average depths of 5, 15, and 25 cm, respectively. To study any seasonal differences, samples were taken in February 2019, and June 2019. Surface samples were collected by a stainless-steel scoop. Samples were stored in glass containers at -20°C after collection to avoid biodegradation of PAHs.

2.2 Extraction of PAHs

PAHs were extracted by microwave-assisted extraction (MAE) (MARS 6, CEM, City, U.S.), based on the EPA SW-846 Test Method 3546 (EPA, 2007). The samples were first air dried for 24 hours in a fume hood. The dried samples were ground and weighed to approximately 5 g (exact weight was recorded), and then introduced into Teflon extraction vessels (100 mL, CEM, Matthews, U.S.). In vessels used for background (blanks), 5 g of clean sea sand (Merck, U.S.) was used. The samples and blanks were extracted in triplicate. For MAE, 30 mL of n-hexane (HPLC grade)-acetone (HPLC grade) (1:1) (v/v) was added to the extraction vessels, followed by 10 µL (100 mg/L)of deuterated PAHs, specifically Naphthalene-d8, Acenaphthene-d10, Phenanthrene-d10,

Chrysene-d12, and Perylene-d12 (AccuStandard, New Haven, U.S.) were used as surrogate standards. MAE was performed at 115℃ for 10 min at 1000 W. After extraction, the vessels cooled to room temperature and the solution was transferred with a pipette into 60 mL amber vials. Residues were rinsed by 5 mL of hexane, hexane-acetone (1 mL) and acetone separately, and the supernatants were transferred to amber vials. Then, the extracts were concentrated to 1 mL by a N-EVAP Nitrogen Evaporator (Organomation, Berlin, U.S.).

2.3 Cleanup of extracts

After extraction, the extracts were cleaned in an alumina column according to EPA publication SW-846, method 3630C (EPA, 1996). Before cleanup, Alumina (Fisher Scientific, Pittsburgh, U.S.) was baked at 450℃ for 24 hours to remove organic matter. The activated alumina was then placed in a desiccator and cooled to room temperature. At this point the alumina was deactivated by adding 3% DI water and it was subsequently equilibrated in the desiccator for 16 hours. Sodium sulfate (Fisher Scientific, Pittsburgh, U.S.) was a baked at 450℃ for 4 hours, then placed in a desiccator. To make extraction columns, glass wool (Acros Organics, Morris Plains, Germany) was placed at the bottom of 10 mL glass disposable pasteur pipets (Pyrex, Corning, U.S.), followed by 5 g of prepared alumina. A layer of sodium sulfate was added at the top of the column to remove potential water from the extracts. The column was rinsed with 20 mL hexane prior to cleaning the PAH extracts that were added at the top of column. The container of

extracts was rinsed with 20 mL hexane-dichloromethane (3:2) (v/v) and transferred to the column. The effluent containing PAHs was collected in a graduated centrifuge tube, which was then concentrated to less than 1 mL by a N-EVAP Nitrogen Evaporator (Organomation, Berlin, U.S.). The cleaned extracts were spiked with 10 µL internal standards mixture (100 mg/L) (Anthracene-d10, Benzo[a]pyrene-d12) (VWR, Radnor, U.S.). Hexane (HPLC grade) was added to the effluent to produce a final volume of exactly 1.0 mL. The samples were vortexed for 10 s to ensure mixing, then loaded onto the GC for GC/MS analysis.

2.4 GC/MS analysis

The analysis method was based on EPA method SW-846 8207. Samples were analyzed by gas chromatography/mass spectrometry (GC-MS) (7890B, Agilent Technologies, U.S.) with an Agilent fused silica capillary column (HP-5ms) and a mass spectrometer detector (5973N, Agilent Technologies, U.S.), which operated in the SIM and Scan mode. The carrier gas was helium, and the injection was in splitless mode with a volume of 1 µL. The temperature of the oven was raised from 70°C to 180°C at 7°C min^{-1}, from 180°C to 225°C at 1°C min^{-1}, from 225°C to 285°C at 5.8°C min^{-1} with isothermal hold at 285°C for 20 min, then ramped to 300°C at 11.5°C min^{-1} and held at 300 °C for 10 min. Target compounds were purchased from AccuStandard (New Haven, Connecticut, U.S.).

2.5 Quality Control

To avoid contamination of the samples, all the containers were made by glass or PTFE. Glassware was cleaned using hexane, methanol, and DI water, and baked at 550℃ for 4 hours before any use in experiments. To avoid contamination between extractions, Teflon extraction vessels were ultrasonicated with hexane and methanol and then rinsed with DI water after sonication. To avoid contamination in the GC-MS column, a hexane injection was added at the first and last of the sequence of run. The recoveries for PAHs were determined by five surrogate standards, Napthalene-d8, Acenaphthene-d10, Phenanthrene-d10, Chrysene-d12, and Perylene-d12, and the recoveries were used to correct the measured concentration of PAHs. Naphthalene-d8 was used to correct the concentration of NAP. The recovery of acenaphrhene-d10 was used to correct the concentration of ACY, ACE and FLU. PHE, ANT and FLA were corrected by phenanthrene-d10, PYR, BaA and CHR were corrected by chrysene-d12. perylene-d12 was used to correct BbF, BkF, BaP, INP, DBA and BPY. The average recoveries of each surrogate standard were calculated, which were 105.90%, 119.35%, 84.53%, 55.87%, and 73.71% for naphthalene-d8, acenaphrhene-d10, phenanthrene-d10, chrysene-d12, and perylene-d12 respectively. Anthracene-d10 was used as internal standard for NAP, ACY, ACE, FLU, PHE, ANT and FLA, and benzo[a]pyrene-d12 was used as internal standard for PYR, BaA, CHR, BbF, BkF, BaP, INP, DBA and BPY (Table 3). The instrument detection limits (IDL) for the tested PAHs ranged from 0.0001 to 0.002 μg/g (Table 4), which were calculated by dividing the instrument detection limits by the sample masses.

The values lower than instrument detection limits were calculated as IDL/2 (EPA, 2006).

2.6 Data analysis

Five-point calibration curves for 16 PAHs, with concentrations ranging from 0.01 to 5 μg/g and R^2>0.98, were used for quantification. To evaluate if significant differences were present among the sampling sites, depths, and seasons, respectively, student t-tests were performed. The confidence level was set at 0.95, and RStudio was used for statistical analysis (REF). Benzo[a]Pyrene Total Toxicity Equivalent (BaP-TEQ), was calculated by multiplying benzo[a]pyrene toxic equivalence factors (BaP-TEFs) and individual PAH concentrations; these values were used to represent the toxicity of total PAHs present in the samples. PAHs and their corresponding BaP-TEFs are showed in Table 3. The calculation follows formula 1.

$$TEQ_i = \sum_{i=1}^{n} C_i \times TEF_i \quad (1)$$

Where i (i = 1⋯16) described the type of PAH, TEQ stands for the calculated BaP-TEQ for samples, C_i is the corresponding concentration of PAH_i, TEF_i is the the value of BaP-TEF for PAH_i.

2.7 DNA extraction and quantification

DNA of positive control cultures (Pseudomonas putida and Pseudomonas fluorescens) were extracted by UltraClean Microbial DNA Isolation Kit (QIAGEN, Hilden, Germany). DNA of bioretention cell media were extracted from 250 mg samples using a DNeasy PowerSoil Kit (QIAGEN, Hilden, Germany) according to manufacturer's

instruction. Nanodrop 2000 (Thermo Scientific, Waltham, U.S.) was used to quantified extracted DNA.

2.8 PCR amplification

Universal primers 341F and 907R were used to amplify the 16S rRNA gene. PAH-ring hydroxylating dioxygenases (PAH-RHDs) and PAH-ring cleaving dioxygenases (PAH-RCDs) primers were used to amplify the functional gene of dioxygenase PAH degradation, and primer pairs are listed in Table 5. PAH-RHD GN and GP primers were work for gram negative and positive bacterial, respectively. There were three primers for PAH-RCDs, namely protocatechuate-3,4-dioxygenase (pca H), catechol-1,2-dioxygenase (C12O) and catechol-2,3-dioxygenase (C23O). DNA samples were stored at -20 ℃.

For PCR reaction, 10.2 μL of nuclease-free water (Ambion, Austin, U.S.), 12.5 μL Dream Taq Green PCR Master Mix (Thermo Scientific, Waltham, U.S.), 0.15 μL of forward and reverse primers (Integrated DNA Technologies, Coralville, U.S.), and 2 μL of template DNA were mixed. AT100 Thermal Cycler (Bio-Rad Laboratories, Hercules, U.S.) was used for PCR analysis. The following thermal cycling conditions were used for PCR amplification: initial denaturation 95 °C for 3 min; 35 cycles of denaturation 95 °C for 30 s, annealing 30 s at annealing temperatures of primers (Table 5), extension 3 min at 72 °C; and a final extension step at 72°C for 10 min. Fragments of 16 S rRNA gene and functional gene of aerobic PAH degradation were separated by gel electrophoresis. 1.5% agarose gel was made by 1.8 g agarose, 120 mL 1X TAE buffer, and 2 drop of 0.625

mg/mL ethidium bromide (Genesee Scientific, San Diego, U.S.). 5 μL of PCR products were loaded to gel and run at 100 V until the dye line was 80% ranging from the wall. After the gel electrophoresis, the digital pictures of gels were obtained and analyzed by FlourChem FC3 (ProteinSimple, San Jose, U.S.).

3. Results and Discussion

3.1 Total PAH concentrations and spatial distribution of PAHs

Quantifiable concentrations of the 16 EPA listed PAHs were detected at all sampling sites; the total PAH concentration ranged from 1.6±0.31 to 25.5±0.14 μg/g. The lowest concentrations of total PAHs in surface samples was detected at 0 m in February 2019(9.7±1.8 μg/g), and the highest value was found at 2.74 m in June 2019 (16.1±0.6 μg/g). The total PAH concentration of the control samples were 1.5±0.5 μg/g in February and 1.2±0.4 μg/g in June, similar to the lowest concentration in the bioretention cell and approximately 10 times lower than the concentrations of surface samples in the bioretention cell (Figure 3). Without the added impact of stormwater, PAHs in the control samples were mainly accumulated by wet and dry deposition. This result indicates that the major accumulation of PAHs in the bioretention cell originated from input delivered via stormwater.

The concentrations of PAHs in the sampling sites were compared by t test, and the results showed that total PAH concentrations of 2.74 m sampling site at June was

significantly higher than that at other sampling sites, and at February the total PAH concentration of 2.74 m was significantly higher than 0.91 sampling site ($p<0.05$). Also, the total PAH concentration at 1.83 m in February was significantly higher than that at 0 and 0.91 m ($p<0.05$). The p-values were showed in appendix. Statistical evaluation of the concentration at other sampling sites didn't show any significant differences. Furthermore, seasonal differences in the concentration of PAHs in the surface samples were not observed ($p>0.05$).

If the sampling point at 0m is not considered, the total PAH concentration was positively correlated with distance, and the correlation coefficients in February and June were 0.862 and 0.966, respectively (Figure 4). The distribution of PAHs in particles of different sizes may be the reason for the increase of PAH concentrations with distance. Herngren (2010) studied the distribution of PAHs with particle size in stormwater (< 0.45μm, 0.45-75μm, 75-150μm and > 150μm), and the highest PAH concentration was found in the 0.45-75μm particles. The distribution of PAH in particles of different sizes may be the reason for the increase of PAH concentration with distance. Large particles tend to be deposited at the inlet of the bioretention cell, while most PAHs will be transported by the stormwater with the fine particles and deposited at a lager distance. The PAH concentrations in core samples together with the distributions showed in Figure 6. At the 0.91 m sampling site, the average of the total PAH concentrations increased with the depth of the core samples, but there was not a statistical significance ($p>0.05$). At the

1.83 m sampling site, the highest concentrations were found at 5 cm (21.3±1.6 μg/g) in February and 15 cm (25.5±1.7 μg/g) in June. Total concentrations had a decreasing trend at 2.74 m in both February and June. The same bioretention cell was studied in 2007-2008 by DiBlasi et al. (2008). Here, the results showed that the trends for the 2.74 m location was similar with regard to the total PAH concentrations in core samples at 1.5 m of this study, the surface samples had the highest PAH concentrations and the concentrations decreasing with the increasing of depth. The core samples at 0.91 m and 1.83 m have the concentrations higher than 1.5 m core samples in 2008 (2.96 μg/g in the top 10 cm segment, 0.33−0.64 μg/g in lower segments), but the concentrations of surface samples were in the same range (12.5−22.7 μg/g), this results shows that PAHs were accumulated in core samples during past 10 years.

Concentrations of PAH concentrations in stormwater management facilities reported by other studies is provided in Table 6. The PAH concentrations among studies vary greatly; the highest value was 89.4 μg/g, and the lowest value was 0.064 μg/g. The total PAH concentrations within a study were also had wide ranges. In a study of sediments from stormwater management ponds at Baltimore, the highest total PAH concentration was 88.9 μg/g and the lowest value was lower than detection limit (0.214 to 4.280 μg/kg, depending on the PAH). One reason for the variations of PAH concentrations may be the surrounding environment of the sampling sites. The relatively high level of PAH concentrations of sediments from stormwater management ponds in Baltimore may due

to the residential and commercial development of surrounding area in the 20 years before the study (Gallagher et al., 2011). Concentration of total PAH was elevated after coal-tar based sealcoat was applied in the watershed (10.9-95.7 μg/g), compared with the concentration before coal-tar based sealcoat was applied (0.54-3.08 μg/g) (Watts et al., 2010). Weinstein (2010) detected the highest PAH conceration from a commercial area (10.4 ± 3.9 μg/g), and relatively lower concentrations were detected at a golf course (0.42 ± 0.22 μg/g), high density residential ponds (347 ± 29 μg/kg), and low density residential area (0.347 ± 0.029 μg/kg).

3.2 Individual PAH concentrations

The concentrations of individual PAHs ranged widely in the bioretention cell media (Figure 6). The 16 EPA listed PAHs were detected in all samples, and the average concentrations of individual PAHs were ranged from 3.68 μg/g to lower than detection limit (0.0001 μg/g for ACE). Individual PAHs were sorted from highest to lowest by average concentration in all depths and distances. Benzo[g,h,i]perylene was the PAH with highest average concentration in February (1.8±0.79 μg/g), while pyrene had the highest average concentration in June (1.8±0.80 μg/g). The lowest concentration was found for acenaphthylene (0.007±0.14 μg/g in February and 0.014±0.014 μg/g in June). PAHs concentration rankings were same in February and June after CHR, and concentrations of same PAH had no significant differences between February and June ($p>0.05$).

3.3 PAHs sources analysis

The 16 EPA listed PAHs were divided into groups according to the ring number: 2-ring (NAP), 3-ring (ACY, ACE, FLU, PHE, ANT), 4-ring (FLA, PYR, BaA, CHR), 5-ring (BbF, BkF, BaP, DBA), and 6-ring (IDP, BPY). PAHs below the 4-ring were classified as LMW-PAH, and PAHs of 4-ring and above were classified as HMW-PAH (Brown and Peake, 2006). In February and June, HMW-PAH contributed 93% to the total PAH concentrations. Furthermore, the results showed that the 4-ring PAHs accounted for the largest part of total PAH (38.8%) of total PAH concentration in February and 39.8% in June. The second highest group contributing to the total PAH concentration was 5-ring PAHs (29.3% in February and 27.9% in June). (Figure 7). Ring-based PAHs distributions did not show significant seasonal differences ($p>0.05$). This suggests that there is no seasonal variation in the source of PAHs, which is discussed in more detail with diagnostic ratios.

Most of the PAHs in the bioretention cell media were HMW-PAH (Figure 7). HMW-PAHs are less volatile, leachable and degradable, so HMW-PAH are more stable in the environment of a bioretention cell (Watts et al., 2010). The high proportion of HMW-PAH may also be due to the sources of PAHs. Lee (1995) studied PAHs in the urban ambient air (traffic-sources) in which concentrations of CHR, BaA, BbF. BkF, BaP, INP, DBA, and BPY were 7.8 times and 16.5 times higher than the concentrations in urban and rural site. Also, a study of highway stormwater runoff in Los Angeles showed that in traffic-sources runoff 4 to 5 ring PAHs account for 97% of total PAHs (Lau et al., 2009).

In a study of impervious surface run-off in Shanghai, China, there were 82.3% HMW-PAH vs. 17.7% LMW-PAH in the stormwater from asphalt road run-off at urban area (Hou et al., 2013). Stormwater in the campus of University of Maryland contained 77% HMW-PAH 2007-2008 (DiBlasi et al., 2008), which was lower than the proportion of HMW-PAH (93%) in the media in this research. This result shows that the accumulation rate of HMW-PAH is faster than that of LMW-PAH, and this may be caused by the relatively lower bioavailability and higher K_{ow} of HMW-PAH. DiBlasi also found that in the bioretention media 90% to 94% of total PAHs were HMW-PAH, which shows that the proportion of HMW-PAH did not change in the past 10 years. In addition, 6-ring PAHs were more prevalent in the bioretention media than in control samples (11.3% in February and 15.8% in June of control samples), since PAHs in the control samples mainly originate from dry and wet deposition of the atmosphere, and most of the PAHs in the bioretention media were input by stormwater transportation.

PAHs with two or three rings are primarily generated by petrogenic sources, whereas PAHs generated by incomplete combustion are composed by PAHs with four to six aromatic rings (Pies et al., 2008). Diagnostic ratios, which is the specific ratio of PAHs and isomer, can be used to identify the sources of PAHs. For example, the ratio of FLA / (FLA + PYR) can distinguish petrogenic (<0.4) and pyrogenic sources (>0.4) (Galarneau, 2008; Yunker et al., 2002; Yunker et al., 2012). BaA/(BaA+CHR), FLA/(FLA+PYR) and ANT/(ANT+PHE) were three diagnostic ratios calculated (Table 7). For each diagnostic

ratio, a PAH isomer with less thermodynamic stability is used in the numerator. As a result, the higher the diagnostic ratios the more combustion-derived PAHs in the samples (Yunker et al., 2002; Yunker et al., 2012). Diagnostic ratios were applied in bivariate form (Figure 8).

The results from the source analysis suggest that PAHs in most bioretention media sampling points were generated by a mix of petroleum sources together with fossil fuel combustion source. No significant difference between February and June was found for both FLA/(FLA+PYR) and BaA/(BaA+CHR) ($P>0.05$). So, there was no seasonal trend when evaluating the sources. The bioretention cell collected stormwater from a drainage area with impervious surfaces such as parking lots and campus roads, thus major sources of PAHs may be leakage of oil and incomplete combustion of fossil fuel. These results are consistent with the results of individual PAH concentrations, which showed that BPY and PYR had the highest concentrations in the bioretention cell (Figure 5). BPY and IND sources are typically caused by gasoline emission and combustion of heavy oil (Iwegbue et al., 2019; Kwon and Choi, 2014; Larsen and Baker, 2003), whereas PYR, BaA, CHR, BbF, BkF, IND, and DBA are markers for diesel emissions (Kwon and Choi, 2014; Wang et al., 2013; Yang et al., 2013).

Results of the three diagnostic ratios in February show (BaA/(BaA+CHR) <0.35, FLA/(FLA+PYR) <0.4, ANT/(ANT+PHE) < 0.1) and two diagnostic ratios (BaA/(BaA+CHR) < 0.35, FLA/(FLA+PYR) < 0.4) in June showed that PAHs from a

petroleum source or mix sources was observed at the 0 m sampling point. The diagnostic ratios had no seasonal difference (Figure 8A), but there were differences in the source ratios between depths of the collected samples. For both ANT/(ANT+PHE) and BaA/(BaA+CHR), the samples at 0 cm were significantly lower than the samples at 15 cm and 25 cm ($p<0.05$), and the samples at 5 cm were also significantly lower than the samples at 15 cm and 25 cm ($p<0.05$), p values are showed in appendix table A3.

The source of PAHs in the surface samples originated from a petroleum source, and as the depth increases, the source of PAHs changed to be from a combustion source (Figure 8B). Due to the filtration of the media, the suspended particles was concentrated at the inlet of the bioretention cell and surface of the media (DiBlasi et al., 2008). As a result, petroleum source PAHs may mainly input into the bioretention cell through suspended particles in stormwater. This may be the reason for the observation of more PAHs originating from a petroleum source at the surface and the inlet of bioretention cell. The source of PAHs in the control samples were derived from a combustion source and were different from the source of PAHs in the bioretention media. This indicated that the PAH content of the petroleum source in the stormwater was higher than that in the atmosphere.

3.4 Toxicity

To assess the effect of the bioretention media on the ecosystem, the concentrations of total PAH and individual PAHs were compared with threshold effect concentration (TEC)

and probable effect concentration (PEC) as a measure of toxicity (MacDonald et al., 2000).

TECs and PECs were determined by the survival or growth of sediment-dwelling organisms in the sediments from aquatic environment (i.e., midge, daphnid, amphipod, bacteria)(MacDonald et al., 2000). If the concentrations of PAHs were higher than PECs, it will have an adverse effect on the survival of the bacteria, which in turn may affect the effect of bioremediation. Since there are no PECs and TECs established for the soil at the moment, and the media in the bioretention cell is similar to the sediments in the aquatic environment, it is assumed that PECs and TECs of sediments are equally effective for bacteria in the media.

Comparison of PAH concentrations with TECs and PECs showed that that mean concentrations of PYR (1.78 μg/g) and CHR (1.40 μg/g) were higher than PECs (Table 8), which means that toxicity of those two PAHs will be observed in the bioretention cell. FLA, PYR, BaA, CHR, and BaP, had the highest concentrations higher than their PECs. As a result, the toxicity of those PAHs will be observed at specific sampling site where FLA, PYR, BaA, CHR, and BaP had the highest concentrations. The highest value of total PAH concentration (25.5 μg/g) was higher than PEC (22.8 μg/g) thus the risk of toxicity caused by the 16 EPA listed PAHs at this sampling point (1.83 m, 15cm depth in June) was present. In contrast, total PAH concentrations in both control samples were lower than TEC, so adverse effects were not expected to occur. Those results show the

negative environmental impact of stormwater with input of PAHs into the bioretention cell with subsequent PAH accumulation in the media. The average concentrations of pyrene and chrysene in all samples were higher than PECs, which shows that these two PAHs in the bioretention cell will affect the survival of bacteria. At 1.83m in June, the total PAH concentration at 15cm depth is greater than PEC, which means that at this sampling point, the survival of bacteria will be affected by the total PAH concentration. This result shows that when bioremediation is used to remove PAHs in media, the effect of PAHs concentrations should be considered.

Other studies have reported similar effects. Howitt (2014) reported that stormwater collected from surrounding residential and commercial districts and highway caused accumulation of PAHs in sediments of a semi-natural wetland in Victoria, Australia. Various PAHs with concentrations exceeded PCEs, which indicate that the toxicity can be observed, were found at the sampling site with highest PAH concentrations (ACE: 0.62 μg/g, PHE: 1.8 μg/g, FLA: 3.9 μg/g, PYR: 3.8 μg/g, BaA: 1.8 μg/g, CHR: 1.8, BaP: 1.8 μg/g). A study in Toronto Canada showed that PECs exceeded by PAH concentrations of sediments (PHE: 1.4 μg/g, FLA: 4.3 μg/g, PYR: 3.3 μg/g, BaA: 1.1 μg/g, CHR: 2.4 μg/g, BaP: 1.6 μg/g) in stormwater management facility (Bartlett et al., 2012). The results of those studies indicates that stormwater causes the accumulation of PAHs, and make the concentrations of PAHs in bioretention media and sediments to exceed PEC.

BaP-TEQs were used in this study to assess the carcinogenic potency of samples in

the bioretention media Eq. (1). BaP-TEQs of surface and core samples in February ranged from 0.22 μg/g to 2.96 μg/g, BaP-TEQs in June ranged from 0.28 μg/g to 3.56 μg/g, and there were no seasonal differences between February and June ($p > 0.05$). The highest values of BaP-TEQs were found at 1.83 m at 5cm depth in February and 1.83 m, 15cm depth in June., The lowest values were found at 2.74 m, 25 cm depth (Table 9).

BaP made the greatest contribution to the total BaP-TEQ, and the average contribution rates was 60.1% (Table 6). Contribution rates of carcinogenic PAHs showed in the decreasing order: BaP (60.09%) > DBA (16.59%) > BdF (9.49%) > INP (8.90%) > BaA (4.34%) > BkF (0.52%) > CHR (0.09%). BaP had the third highest concentration of all carcinogenic PAHs, but it contributed the most to carcinogenicity due to its high BaP-TRQ. This indicated that BaP is the most important carcinogen in the bioretention cell, which means that when assessing the environmental impact of the bioretention cell media, BaP should receive most attention. In soils from an industrial district in Shanxi, China, BaP accounted for 73.7% of the total BaP-TEQ (Jiao et al., 2017) and in surface sediments of San Diego Bay, CA, USA, the contribution rate of BaP for BaP-TEQ was over 90% (Neira et al., 2017). Since the main source of BaP is fossil fuel combustion by motor vehicle (Dickhut et al., 2000), the carcinogenicity of media in the bioretention cell is mainly caused by motor vehicle emissions. This shows that the bioretention cell helps to reduce the pollution of receiving waters by BaP by adsorbing BaP from vehicle exhaust. However, if the concentration of BaP accumulated in the bioretention cell media

is too high, there is also a risk of environmental impact.

3.5 Gradient PCR

Pseudomonas putida and *Pseudomonas fluorescens* were tested as positive control for PAH-RHD GN, C12O and pca H primer, and gradient PCR was performed for its DNA samples to find the optimal annealing temperature for PCR. The annealing temperature range of gradient PCR were 50℃ to 60℃, and automatically divided into eight temperatures by the instrument (50℃, 50.7℃, 51.9℃, 53.8, 56.1, 58.0℃, 59.2℃, and 60℃). The electrophoretic profiles of the gradient PCR are showing in appendix (figure A2 and figure A3). Bands for PAH-RHD GN were not find on the gel for both *Pseudomonas putida* and *Pseudomonas fluorescens*, but bands for C12O (470 bp) and pca H (395 bp) were found for *Pseudomonas putida*. There were error bands, which were around 600 pb and more than 1000 bp, for C12O. The optimal annealing temperature can be determined based on the brightness of the bands. Therefore, the optimal annealing temperature for C12O was between 56.1℃ and 58℃, because the bands for C12O had relatively high brightness and error bands had low brightness. The optimal annealing temperature for pca H was 50 ℃, because the brightness of the band is the highest.

3.6 Gel electrophoresis

PAH-RCDs can promote the degradation of catechol, which is PAH biodegradation intermediate products. C12O gene and pca H gene work for ortho fission and meta fission pathway, respectively(Thomas et al., 2016). The gel electrophoresis analysis revealed the

biodegradability of PAHs in the bioretention media (Figure 9). There are 1 lane for control sample and 12 lanes for media samples. Bands for C12O genes were found for some samples, but pca H gene was not found in the bioretention cell. As a result, bacteria in media may be able to degrade catechol through ortho fission pathway. Bands for C12O were not appeared at S7 (1.83m 5cm), S8 (1.83m 15cm), S11 (2.74m 15cm) and S12 lanes (2.74m 25cm). This result is consistent with the dioxygenase degradation pathway of PAHs. Because this pathway is an aerobic pathway, the lack of oxygen deep in the media makes this degradation pathway difficult. The degradation of catechol by PAH-RCDs is one of the key steps in the biodegradation of PAHs, but only the presence of the PAH-RCD genes in media does not determine that PAH can be biodegraded in bioretention cells. In addition, it is also necessary to determine whether the PAH-RHD genes, which play a role in the first step of PAH biodegradation, exists in media.

The distribution of PAH-RCD genes indicates that the PAH biodegradation of the dioxygenase pathway may not occur in the deep part of bioretention, but these parts still have PAHs that need to be degraded. For example, there was no PAH-RCD gene below 5cm depth at 1.83m, but the total PAH concentrations were even higher than the total PAH concentration of the surface sample. This result reveals the limitations of using the dioxygenase pathway for bioretention cell media bioremediation, that is, this approach may not be possible in the depths of media. Therefore, when performing bioremediation of the bioretention cell, it may be necessary to cooperate with bioventing.

3.7 Recoveries

The calculation of recoveries has influences on the total and individual PAH concentrations and one diagnostic ratio. The distribution of PAHs was hardly affected by recoveries. And the figures and tables without the calculation of recoveries are in the appendix.

Without the calculation of recoveries, the total PAH concentrations were ranged from 1.20 μg/g (2.74 m 25 cm in February) to 19.37 μg/g (1.83m 15 cm in June), which lower than the values corrected by recoveries (Figure A4). There are larger seasonal differences between February and June. Total PAH concentrations in the surface samples at 0.91 m and 2.74m have significant seasonal differences ($p < 0.05$). The highest values of total PAH concentrations in the surface samples still be found at 2.74 m. The distribution of total PAH concentrations in core samples was the same as the values corrected by recoveries (Figure A5).

Because of relatively low recoveries of HMW-PAHs, HMW-PAHs had lower proportion in total PAH concentrations. The proportion of HMW-PAHs reduced form 93% to 92%, and instead of benzo[g,h,i]perylene, pyrene had highest average concentration in June (Figure A6).

The reduction of PAH concentrations also caused less PAH concentrations exceed PECs. Compare with the concentrations corrected by recoveries, the highest concentration of benzo[a]anthracene and total PAH were reduced below PECs, and no

average concentration higher than PEC (Table A4). There was little change in the contribution of carcinogenic PAHs to BaP-TEQs. Benzo[a]pyrene still made most contribution to the total BaP-TEQ, and the proportion was 60.73%.

Recoveries had influence on diagnostic ratio of FLA/(FLA+PYR) because the recoveries of fluoranthene and pyrene were represented by different surrogate standards. Without the correction of recoveries, FLA/(FLA+PYR) has larger values, which indicates coal, wood, and grass combustion source (figure A7). Other ratios were not influenced by recoveries since PAHs on the numerator and denominator had the same surrogate standard.

4. Conclusions and summary

Studies have shown that in the range of this study, the total PAH concentration was in the middle distance and middle depth of the bioretention cell. And through compare the results with the study at the same site in 2008, it is revealed that PAHs accumulated in the core samples during past 10 years. Studies on individual PAH concentrations found that PAHs derived from fossil fuel combustion mainly contributed to total PAH concentrations, which is consistent with the results of PAH source analysis based on the diagnostic ratios. The distribution of PAH toxicity in bioretention cell is similar to the distribution of PAH concentrations, the highest total PAH concentration exceeds PEC, and the concentrations of PAHs in some individuals exceeds PECs, which indicates that PAH toxicity in media is likely to cause environmental impacts. BaP emitted by motor

vehicles mainly contributed to the carcinogenicity in media.

5. Acknowledgements

This study was funded by SERDP Project ER18-C3-1303 to PI Dr. Birthe Kjellerup, University of Maryland, Department for Civil and Environmental Engineering, College Park.

6. Tables and figures

Table 1. 16 priority PAHs identified by EPA

Compound name	Abbreviation	Group of carcinogenic activity by IARC[1]	$LogK_{OA}$	$LogK_{OW}$
Naphthalene	NAP	2B	5.19	3.3
Acenaphthylene	ACY	-	6.23	3.93
Acenaphthene	ACE	3	6.28	3.92
Fluorene	FLU	3	6.58	4.18
Phenanthrene	PHE	3	7.33	4.46
Anthracene	ANT	3	7.09	4.45
Fluoranthene	FLA	3	8.32	5.16
Pyrene	PYR	3	8.8	4.88
Benzo[a]anthracene	BaA	2A	9.1	5.76
Chrysene	CHR	2B	9.4	5.73
Benzo[b]fluoranthene	BbF	2B	10.68	5.78
Benzo[k]fluoranthene	BkF	2B	10.73	6.11
Benzo[a]pyrene	BaP	1	10.86	6.13
Indeno[1,2,3-cd]pyrene	INP	2B	11.56	6.7
Dibenzo[a,h]anthracene	DBA	2A	13.67	6.5
Banzo[g,h,i]perylene	BPY	3	11.77	6.63

[1]Carcinogenic to human beings: (1) carcinogens to human, (2A) probable carcinogens, (2B) possible carcinogens, and (3) evaluation of carcinogenic activity is not possible due to limited data, IARC (2012).

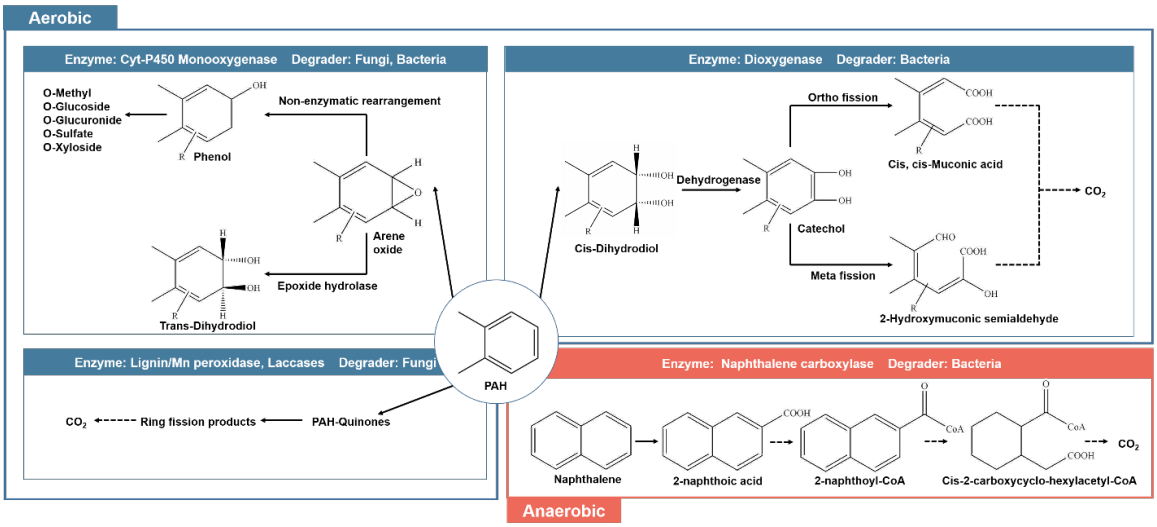

Figure 1. Pathway of PAH biodegradation.

Table 2. Examples of bacteria and fungi that can degrade PAHs

Enzyme	Kingdom	Name of organism	PAH	References
Aerobic				
P450 monooxygenases	fungi	*Phanerochaete chrysosporium*	Aaphthalene, phenanthrene, pyrene, benzo[*a*]pyrene	Syed and Yadav,2012
P450 monooxygenases	Bacteria	*Bacillus megaterium*	Phenanthrene, fluoranthene, pyrene	Carmichael and Wong, 2001
Ligninolytic enzymes	Fungi	*Peniophora incarnate*	Anthracene, phenanthrene, fluoranthene, pyrene	Lee, Jang et al., 2014
Ligninolytic enzymes	Fungi	*Trichaptum abietinum*		
Ligninolytic enzymes	Fungi	*Mycoaciella bispora*		
PAH-RHD	Bacteria	*Pseudomonas salomonii*	Fluorene, phenanthrene, pyrene	Bacosa and Inoue, 2015
PAH-RHD	Bacteria	*Sphingobium amiense*		
PAH-RHD	Bacteria	*Dokdonella koreensis*		
PAH-RHD	Bacteria	*Pseudomonas putida*	Naphthalene, phenanthrene, pyrene	Dutta, Shityakov et al., 2017
PAH-RHD	Bacteria	*Mycobacterium vanbaalenii*	Pyrene, fluoranthene	Darmawan, Nakata et al., 2015
PAH-RHD	Bacteria	*Burkolderia fungorum*		
Anaerobic				
Phenanthrene carboxylase	Bacteria	*Desulfobacteraceae organism*	Phenanthrene	Himmelberg, Brüls et al., 2018
Unknown	Bacteria	*Pseudomonas stutzeri*	phenanthrene, benzo[a]pyrene, fluoranthene	Liang et al., 2014

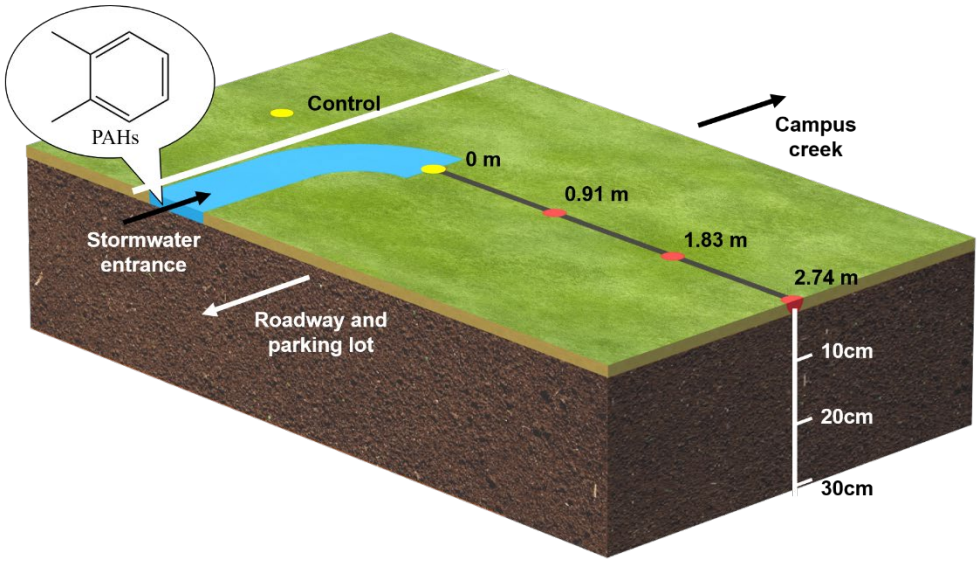

Figure 2. Vertical view of the bioretention cell at UMD (Yellow dot: sampling points for surface samples; red dot: sampling points for surface samples and core samples.)

Table 3. Standards and BaP-TEFs for PAHs

Compound name	Surrogate standard	Internal standard	BaP-TEFs[1]
Naphthalene	Napthalene-d8	Anthracene-d10	-
Acenaphthylene	Acenaphthene-d10		-
Acenaphthene			-
Fluorene			-
Phenanthrene	Phenanthrene-d10		-
Anthracene			-
Fluoranthene			-
Pyrene	Chrysene-d12	benzo[a]pyrene-d12	-
Benzo[a]anthracene			0.1
Chrysene			0.001
Benzo[b]fluoranthene	Perylene-d12		0.1
Benzo[k]fluoranthene			0.01
Benzo[a]pyrene			1.0
Indeno[1,2,3-cd]pyrene			0.1
Dibenzo[a,h]anthracene			1.0
Banzo[g,h,i]perylene			-

[1]Data source: Provisional guidance for quantitative risk assessment of polycyclic aromatic hydrocarbons (EPA, 1993) .

Table 4. IDLs and quantifiable limits of PAHs

Comp #	Compound Name	IDL (ppm)	IDL (µg/g)	Quantifiable Limit (µg/g)
1	Naphthalene	0.0005	0.0001	0.0002
2	Acenaphthylene	0.005	0.001	0.002
3	Acenaphthene	0.0005	0.0001	0.0002
4	Fluorene	0.0005	0.0001	0.0002
5	Phenanthrene	0.001	0.0002	0.0004
6	Anthracene	0.0005	0.0001	0.0002
7	Fluoranthene	0.0005	0.0001	0.0002
8	Pyrene	0.0005	0.0001	0.0002
9	Benzo[a]anthracene	0.005	0.001	0.002
10	Chrysene	0.0005	0.0001	0.0002
11	Benzo[b]fluoranthene	0.005	0.001	0.002
12	Benzo[k]fluoranthene	0.005	0.001	0.002
13	Benzo[a]pyrene	0.005	0.001	0.002
14	Indeno[1,2,3-cd]pyrene	0.01	0.002	0.004
15	Dibenzo[a,h]anthracene	0.01	0.002	0.004
16	Banzo[g,h,i]perylene	0.005	0.001	0.002

Table 5. Primers and target genes for aerobic PAH degrading

Target	Primer	Annealing length (bp)	Annealing temp. (℃)	F/R	Reference
16S rDNA	341 907	586	55	f r	Li et al., 2009
PAH-RHD	PAH-RHD GN	306	57	f r	Cébron et al., 2008
	PAH-RHD GP	292	54	f r	
PAH-RCD	C12O	470	58	f r	Thomas et al., 2015
	C23O	407	58	f r	
	pca H	395	50	f r	

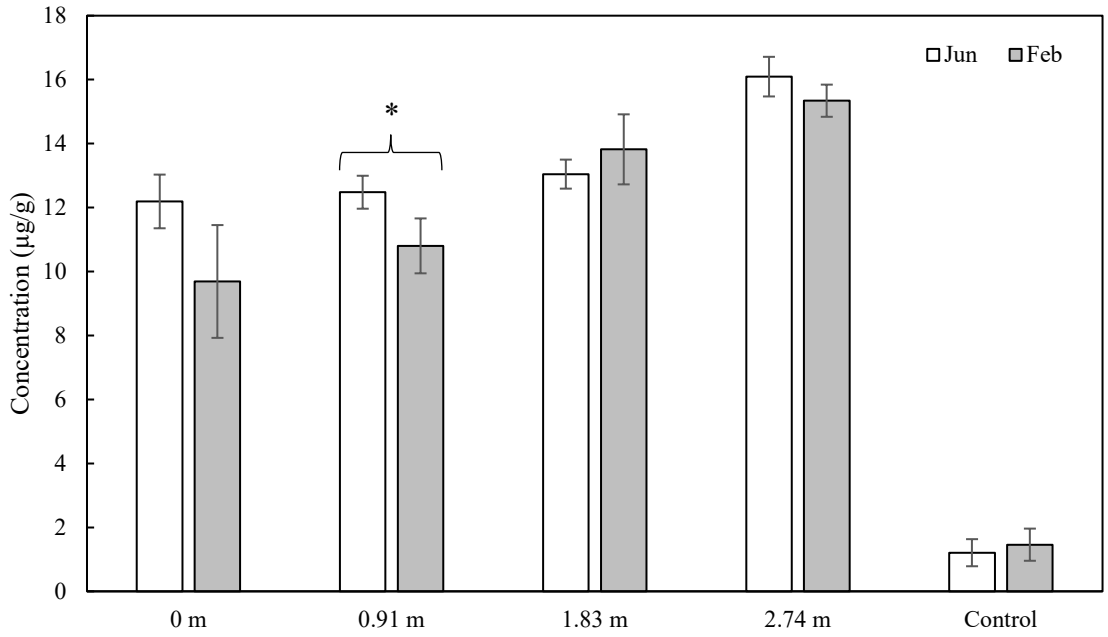

Figure 3. Total PAH concentrations in the surface samples at the bioretention cell (Error bars show the standard deviation of the samples. One star reflects a significance level of at least 0.05 between February and June.)

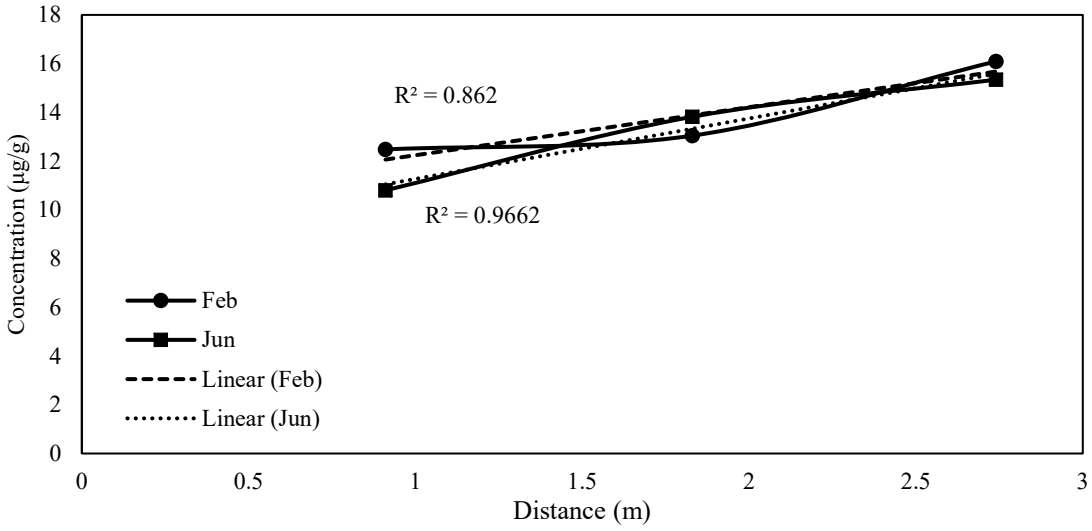

Figure 4. Linear correlation between concentration and distance

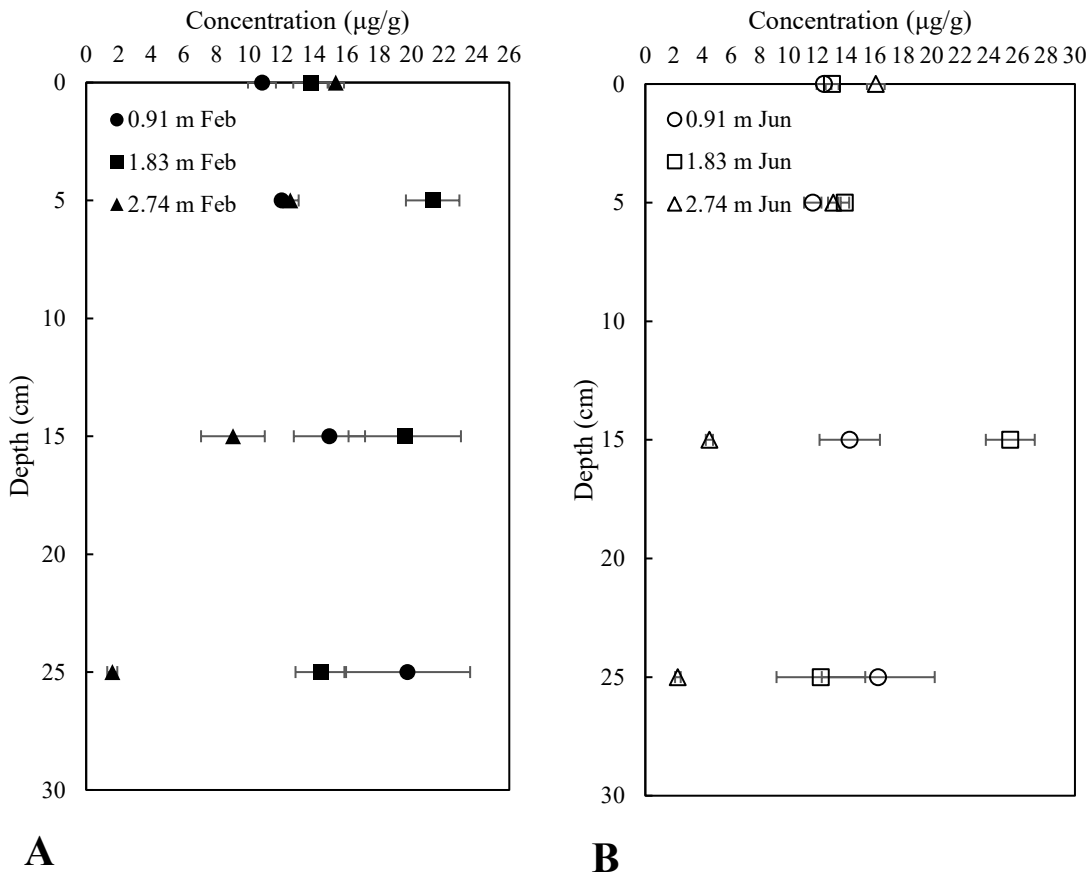

Figure 5. Total PAH concentrations of core samples. A: Total PAH concentration of core samples in February. B: Total PAH concentration of core samples in June (Error bars indicates the standard deviation of the samples)

Table 6. Reported PAH concentrations in stormwater sediments

Location	Year	Sample	Compounds	Range (μg/g)	Reference
Kielce, Poland	2015	Sediments from stormwater drainage system	15 PAHs	39.3-89.4	(Sałata and Dąbek, 2017)
Denmark	2008-2009	Stormwater wet detention ponds	16 PAHs	2.22-0.019	(Istenič et al., 2011)
Toronto, Ontario, Canada	2007-2008	Stormwater management facility sediments	16 PAHs	6.1-20	(Bartlett et al., 2012)
Warrnambool, Victoria, Australia	2008-2009	Wetland sediments impacted by stormwater	16 PAHs	3.02-23.13	(Howitt et al., 2014)
College Park, Maryland, U.S.	2007	Sediments from bioretention cell	16 PAHs	< 22.7	(DiBlasi et al., 2008)
Baltimore, Maryland, U.S.	2007	Sediments from stormwater management ponds	14 PAHs	< 88.94	(Gallagher et al., 2011)
Bergen, Norway	2005	Sediments from stormwater traps	16 PAHs	< 80	(Jartun et al., 2008)
Oxted, Surrey, UK	2002	Stormwater drainage sediments	16 PAHs	33.5-64.5	(Kamalakkannan et al., 2004)
Coastal South Carolina, U.S.	2005-2007	Stormwater detention pond sediments	16 PAHs	0.064-26.29	(Weinstein et al., 2010)
University of New Hampshire	2007-2010	Sediments from a stormwater swale and receiving wetland	16 PAHs	0.54-95.7	(Watts et al., 2010)

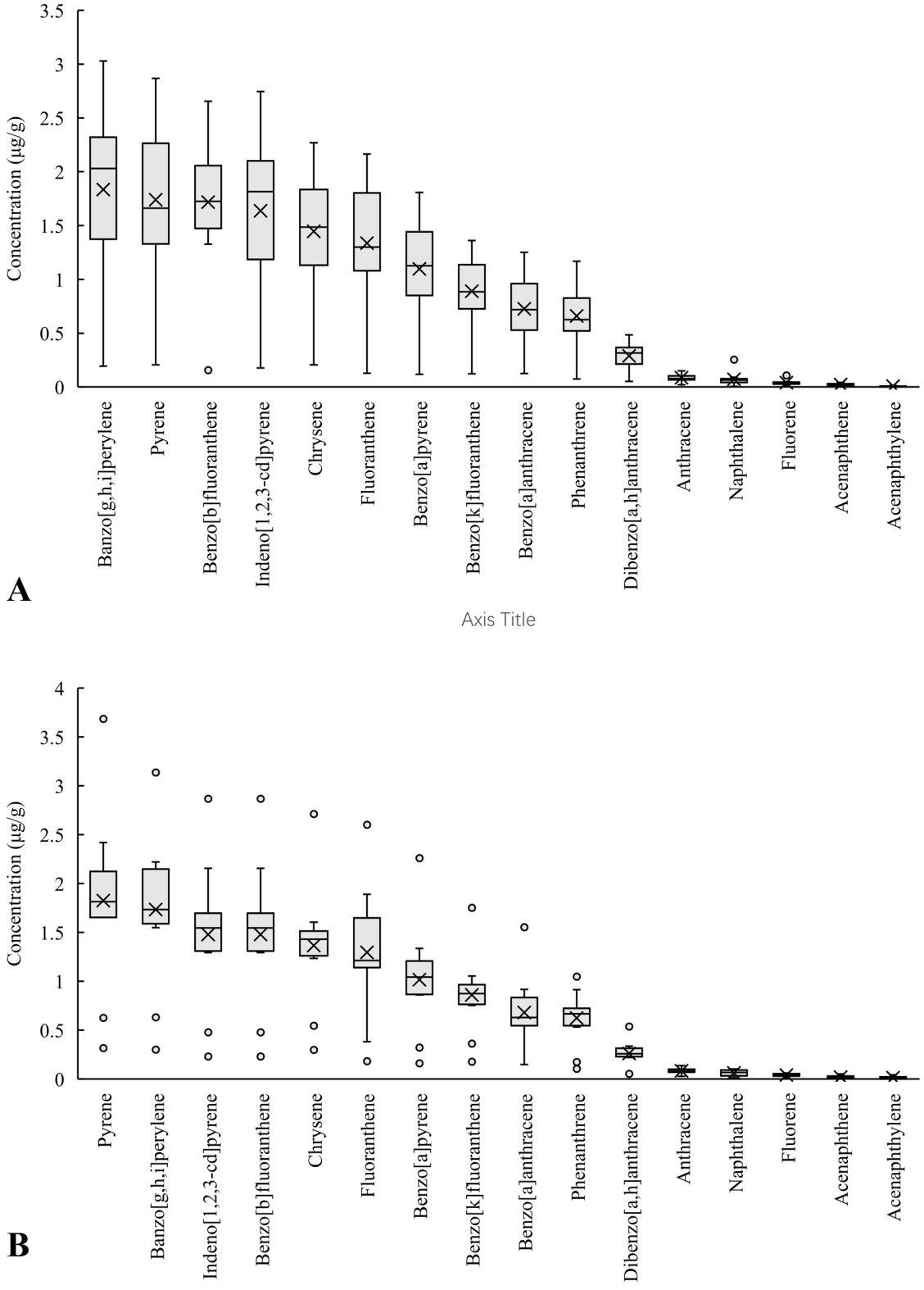

Figure 6. Individual PAH Concentrations in the surface and core samples at the

bioretention cell (A: Concentrations of individual PAHs of samples in February. B: Concentrations of individual PAHs of samples in June. The upper and lower ends of the lines are the maximum and minimum values, the upper and lower ends of the boxes are quartiles, the middle segments of the boxes are the medians, the crosses represent the means, and the dots represent the outliers)

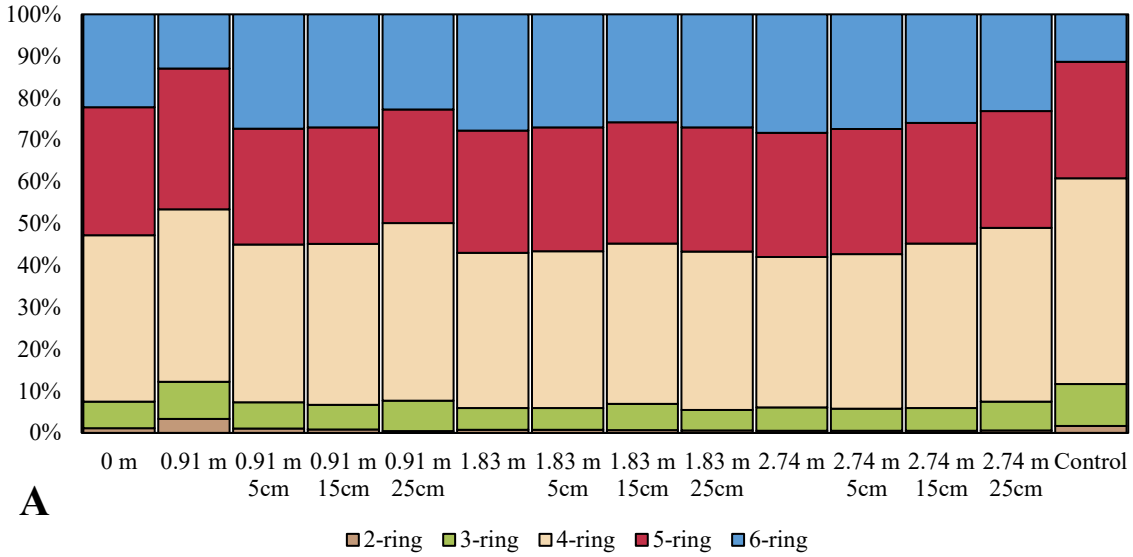

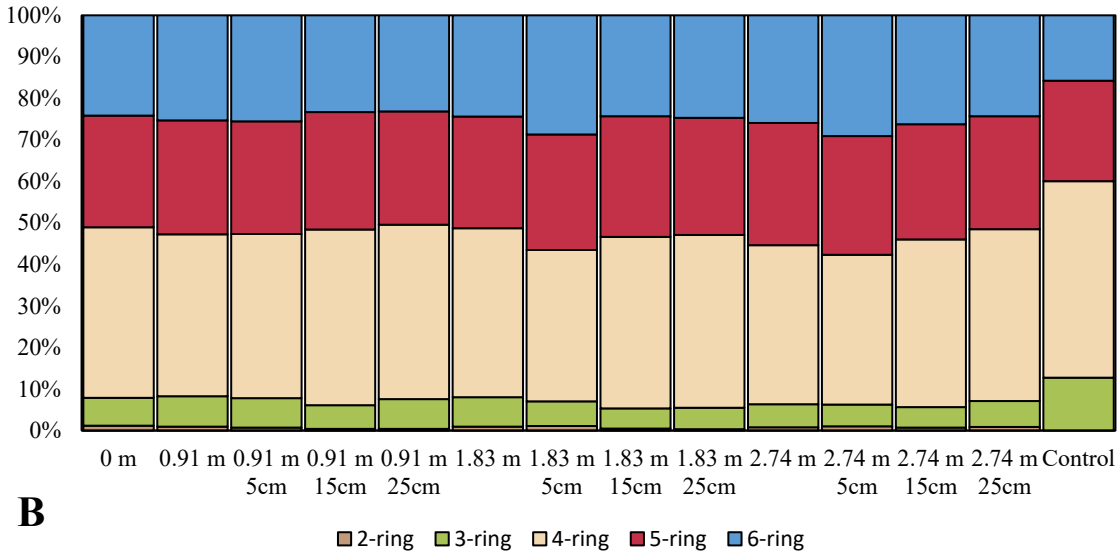

Figure 7. Proportion of 2-ring, 3-ring, 4-ring, 5-ring and 6-ring PAHs in total PAH concentration A: February. B: June

Table 7. Significations of PAH source diagnostic ratios

Diagnostic ratios	Petroleum	Liquid fossil fuel combustion	Grass/wood/coal combustion	References
BaA/(BaA+CHR)	<0.20	>0.35	>0.35	(Yunker et al., 2002; Yunker et al., 2012)
FLA/(FLA+PYR)	<0.40	0.40-0.50	>0.50	
ANT/(ANT+PHE)	<0.10	>0.10	>0.10	

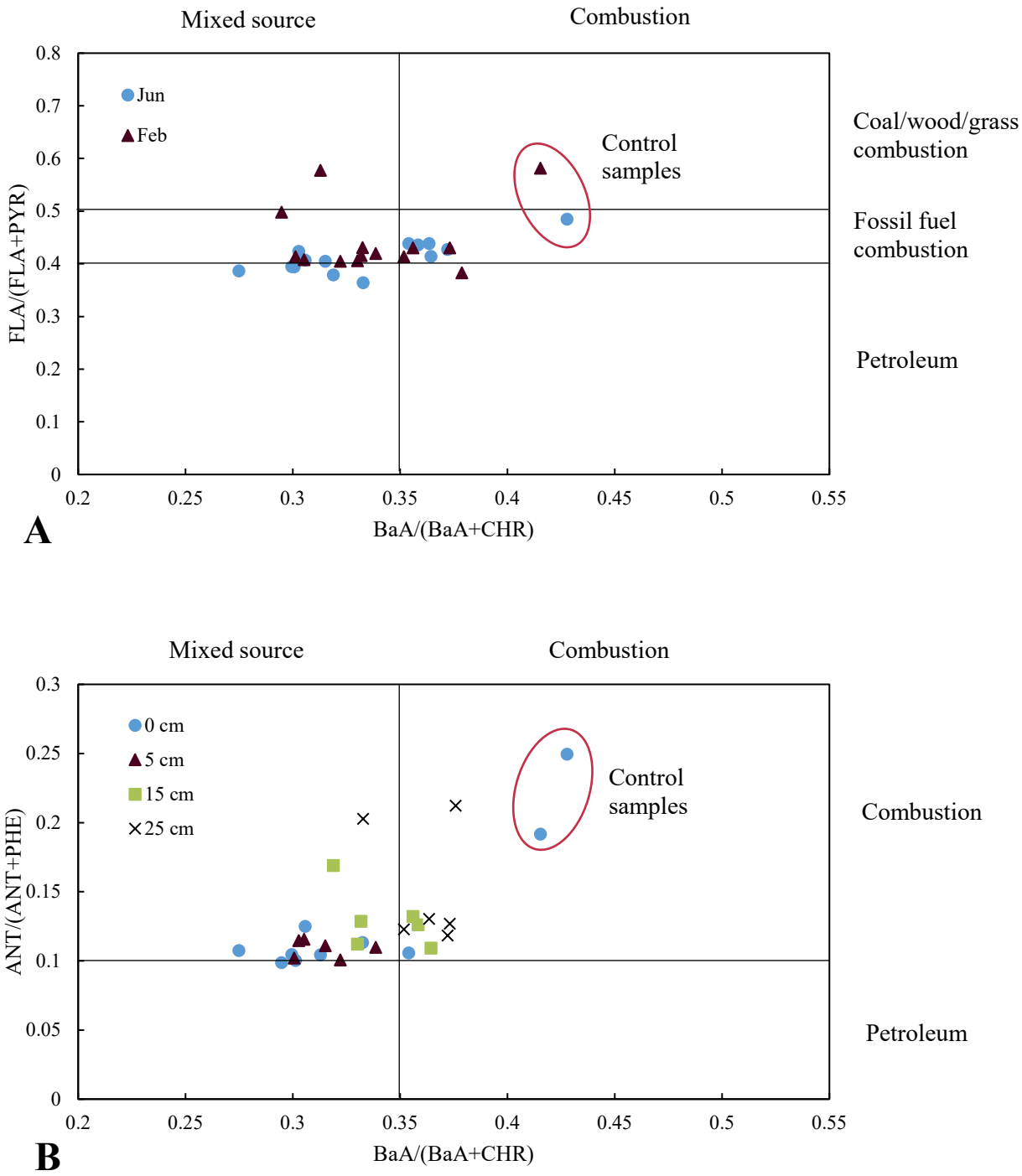

Figure 8. Diagnostic ratios of FLA/(FLA+PYR) against BaA/(BaA+CHR) (A) and diagnostic ratios of ANT/(ANT+PHE) against BaA/(BaA+CHR) (B)

Table 8. Highest, lowest, and mean values of Total PAH and 16 PAHs, and compared with TECs and PECs (μg/g)

Compound name	Highest value	Lowest value	Mean	TEC[1]	PEC[1]	References
NAP	0.2546	0.0065	0.0676	0.1760	0.5610	MacDonald, et al. 2000
ACY	0.0521	<0.001	0.0106	0.0059	0.1280	CCME, 1998
ACE	0.0838	<0.001	0.0205	0.0067	0.0889	CCME, 1998
FLU	0.1065	0.0124	0.0397	0.0774	0.5360	MacDonald, et al. 2000
PHE	1.1692	0.0746	0.6393	0.2040	1.1700	MacDonald, et al. 2000
ANT	0.1701	0.0201	0.0842	0.0572	0.8450	MacDonald, et al. 2000
FLA	2.6018	0.1276	1.3097	0.4230	2.2300	MacDonald, et al. 2000
PYR	3.6839	0.2056	1.7751	0.1950	1.5200	MacDonald, et al. 2000
BaA	1.5541	0.1262	0.6999	0.1080	1.0500	MacDonald, et al. 2000
CHR	2.7115	0.2070	1.3986	0.1660	1.2900	MacDonald, et al. 2000
BbF	2.8661	0.1547	1.5878	0.2400	13.4000	Similar as below[2]
BkF	1.7517	0.1236	0.8686	0.2400	13.4000	Persaud et al. 1993
BaP	2.2591	0.1178	1.0507	0.1500	1.4500	MacDonald, et al. 2000
INP	3.0652	0.1764	1.5712	0.2000	3.2000	Persaud et al. 1993
DBA	0.5358	0.0524	0.2734	0.0330	1.3000	Persaud et al. 1993
BPY	3.1367	0.1948	1.7714	0.1700	3.2000	Persaud et al. 1993
Total PAH	25.4848	1.6031	13.1682	1.6100	22.8000	MacDonald, et al. 2000

[1]Values of TEC and PEC normalized by 1% total organic carbon (TOC) content, assumes that TOC of samples in bioretention cell and control samples were 1%.

[2]There are no guideline values for BbF, assumes that BbF have the same TEC and PEC value with BkF because of the similarity of their chemical structures.

Table 9. BaP-TEQs for carcinogenic PAHs in the media of bioretention cell (μg/g)

Feb	0m 0cm	0.91m 0cm	0.91m 5cm	0.91m 15cm	0.91m 25cm	1.83m 0cm	1.83m 5cm
BaA	0.04	0.05	0.06	0.08	0.13	0.07	0.12
CHR	0	0	0	0	0	0	0
BbF	0.16	0.21	0.13	0.16	0.2	0.17	0.27
BkF	0.01	0.01	0.01	0.01	0.01	0.01	0.01
BaP	0.67	0.8	0.92	1.2	1.64	1.13	1.81
IDP	0.1	0.07	0.15	0.19	0.22	0.18	0.27
DBA	0.17	0.13	0.26	0.32	0.39	0.31	0.48
Total	**1.15**	**1.27**	**1.53**	**1.96**	**2.6**	**1.88**	**2.96**
	1.83m 15cm	1.83m 25cm	2.74m 0cm	2.74m 5cm	2.74m 15cm	2.74m 25cm	Control
BaA	0.11	0.08	0.07	0.06	0.05	0.01	0.01
CHR	0	0	0	0	0	0	0
BbF	0.24	0.18	0.2	0.16	0.11	0.02	0.02
BkF	0.01	0.01	0.01	0.01	0.01	0	0
BaP	1.65	1.24	1.19	1.01	0.72	0.12	0.09
IDP	0.24	0.19	0.2	0.16	0.11	0.02	0.01
DBA	0.42	0.33	0.34	0.28	0.2	0.05	0.04
Total	**2.67**	**2.03**	**2.02**	**1.69**	**1.19**	**0.22**	**0.17**
Jun	0m 0cm	0.91m 0cm	0.91m 5cm	0.91m 15cm	0.91m 25cm	1.83m 0cm	1.83m 5cm
BaA	0.06	0.06	0.05	0.08	0.09	0.06	0.06
CHR	0	0	0	0	0	0	0
BbF	0.14	0.14	0.13	0.16	0.18	0.16	0.16
BkF	0.01	0.01	0.01	0.01	0.01	0.01	0.01
BaP	0.87	0.93	0.86	1.2	1.34	0.93	1.05
IDP	0.13	0.14	0.13	0.16	0.19	0.14	0.18
DBA	0.22	0.24	0.24	0.3	0.34	0.26	0.28
Total	**1.15**	**1.27**	**1.48**	**1.91**	**2.52**	**1.81**	**2.86**
	1.83m 15cm	1.83m 25cm	2.74m 0cm	2.74m 5cm	2.74m 15cm	2.74m 25cm	Control
BaA	0.16	0.08	0.08	0.06	0.03	0.01	0.01
CHR	0	0	0	0	0	0	0
BbF	0.29	0.13	0.22	0.15	0.05	0.02	0.01
BkF	0.02	0.01	0.01	0.01	0	0	0
BaP	2.26	1.05	1.21	1.04	0.32	0.16	0.07
IDP	0.31	0.15	0.2	0.18	0.05	0.03	0.01
DBA	0.54	0.25	0.33	0.28	0.08	0.05	0.02
Total	**2.58**	**1.95**	**1.95**	**1.63**	**1.15**	**0.2**	**0.17**

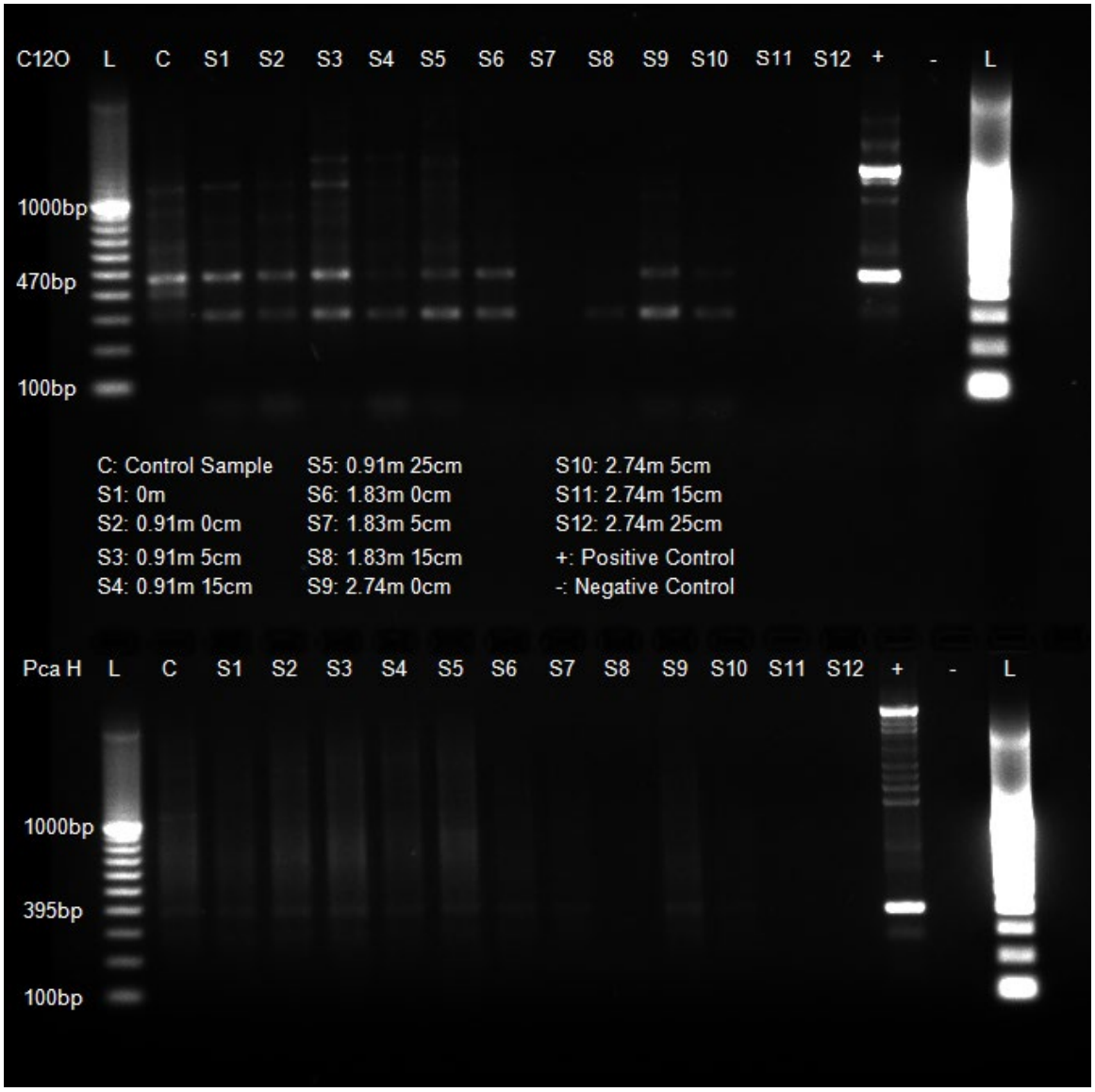

Figure 9. Gel electrophoresis of PAH-RCD genes

7. Appendix

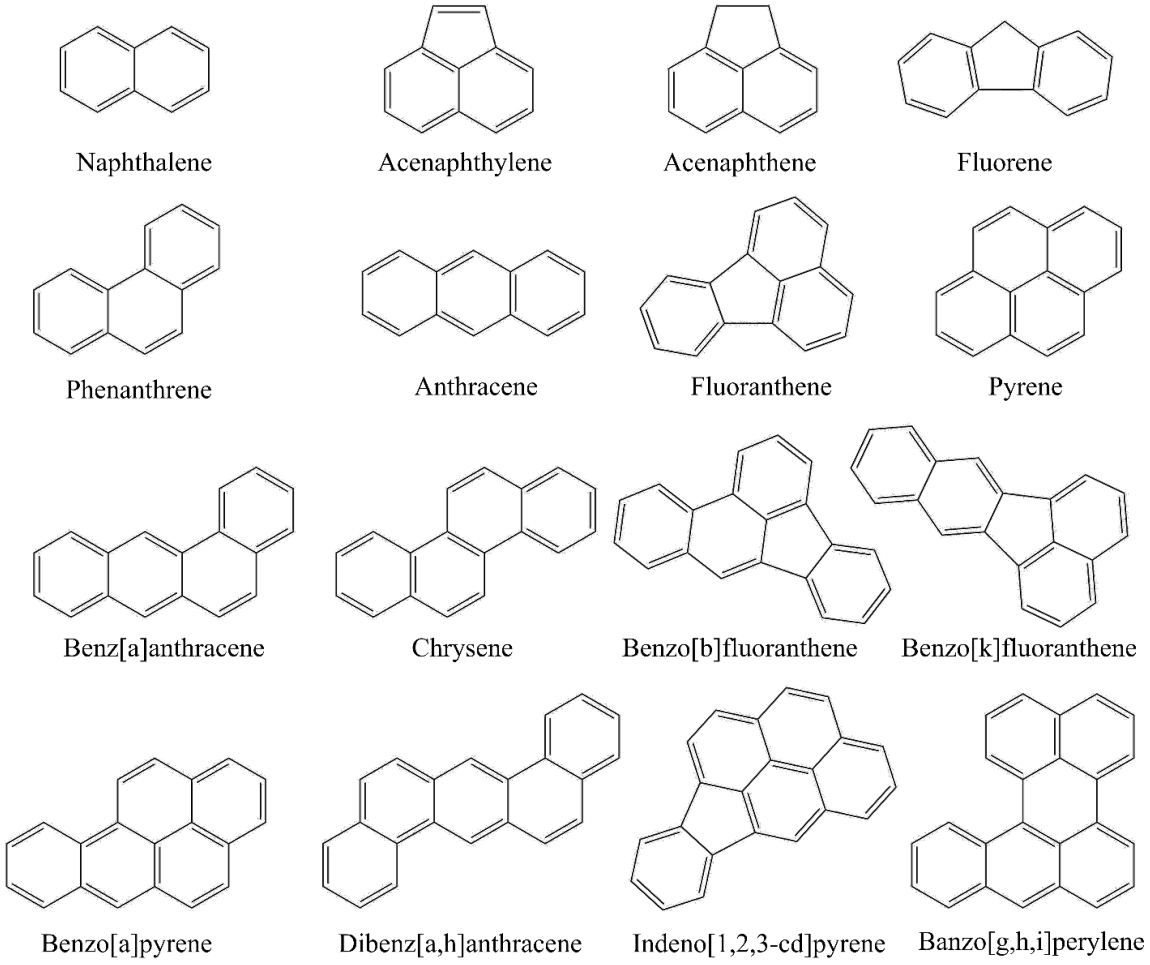

Figure A1. Molecular structure of 16 EPA PAHs

Table A1. Surface samples in February and p-values (H_0: $\mu_{row} = \mu_{column}$, H_A: $\mu_{row} > \mu_{column}$)

February	0 m	0.91 m	1.83 m	2.74 m	C
0 m	0.5000	0.2648	0.0667	0.0615	0.9590
0.91 m	0.7352	0.5000	0.0110	0.0016	0.9998
1.83 m	0.9333	0.9890	0.5000	0.0614	0.9997
2.74 m	0.9385	0.9984	0.9386	0.5000	1.0000
C	0.0410	0.0002	0.0003	0.0000	0.5000

Table A2. Surface samples in June and p-values (H_0: $\mu_{row} = \mu_{column}$, H_A: $\mu_{row} > \mu_{column}$)

June	0 m	0.91 m	1.83 m	2.74 m	C
0 m	0.5000	0.3337	0.1083	0.0019	0.9999
0.91 m	0.6663	0.5000	0.1663	0.0044	0.9990
1.83 m	0.8917	0.8337	0.5000	0.0016	1.0000
2.74 m	0.9981	0.9956	0.9984	0.5000	1.0000
C	0.0001	0.0010	0.0000	0.0000	0.5000

Table A3. Samples with p-value less than 0.05 (H_0: $\mu_1 = \mu_2$, H_A: $\mu_1 < \mu_2$)

	0 cm and 15 cm	0 cm and 25 cm	5 cm and 15 cm	5 cm and 25 cm
ANT/(ANT+PHE)	0.0260	0.0255	0.0325	0.0284
BaA/(BaA+CHR)	0.0061	0.0002	0.0069	0.0002

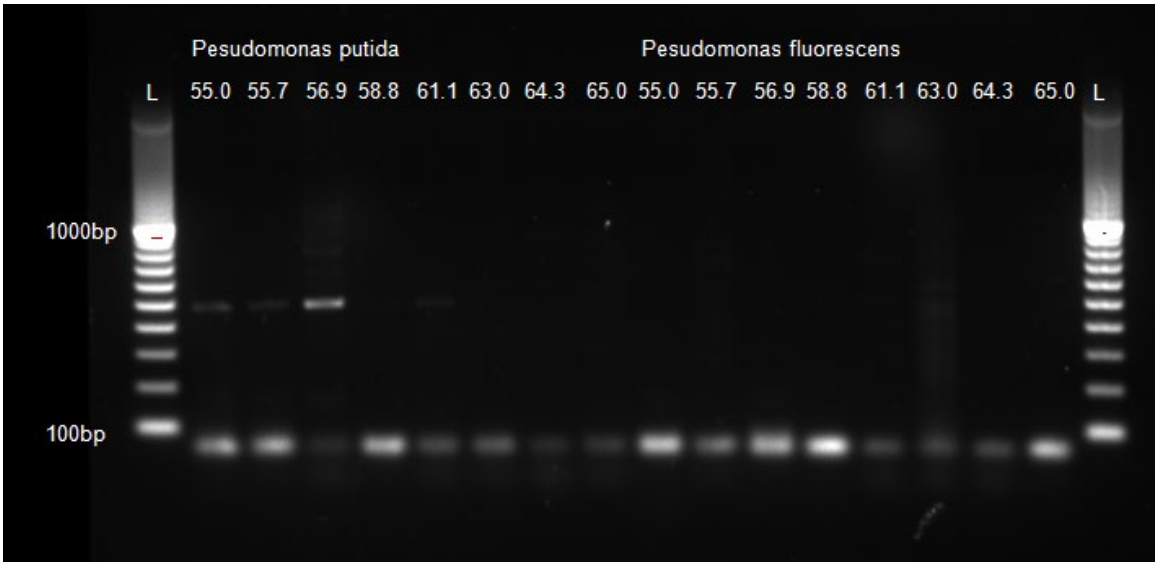

Figure A2. Electrophoretic profiles of PAH-RHD GN

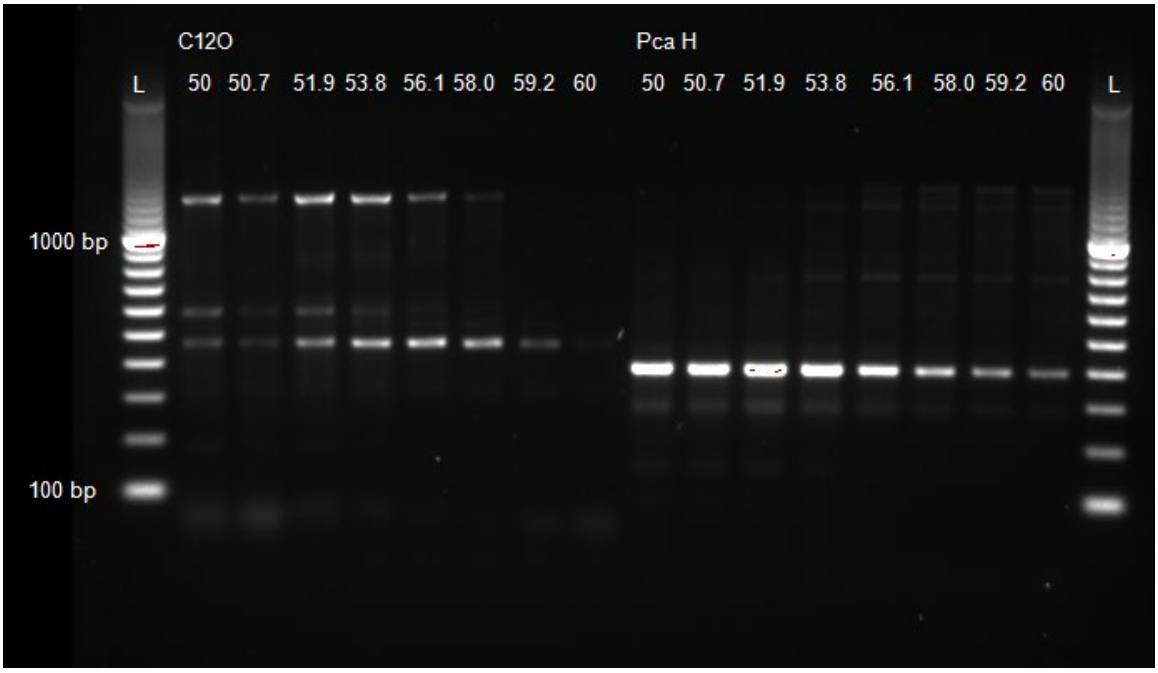

Figure A3. Electrophoretic profiles of C12O and pca H

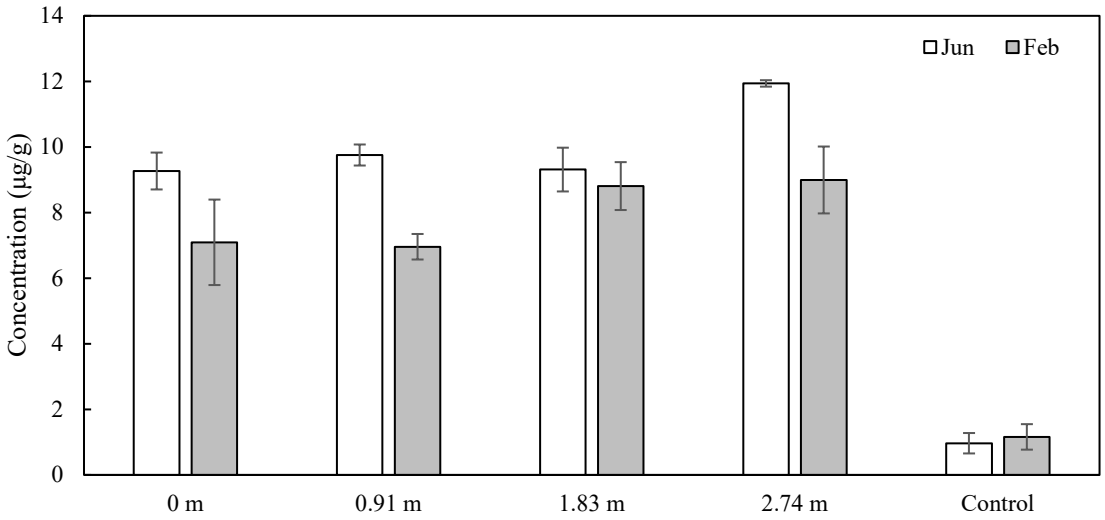

Figure A4. Total PAH concentrations in the surface samples at the bioretention cell (Error bars show the standard deviation of the samples.)

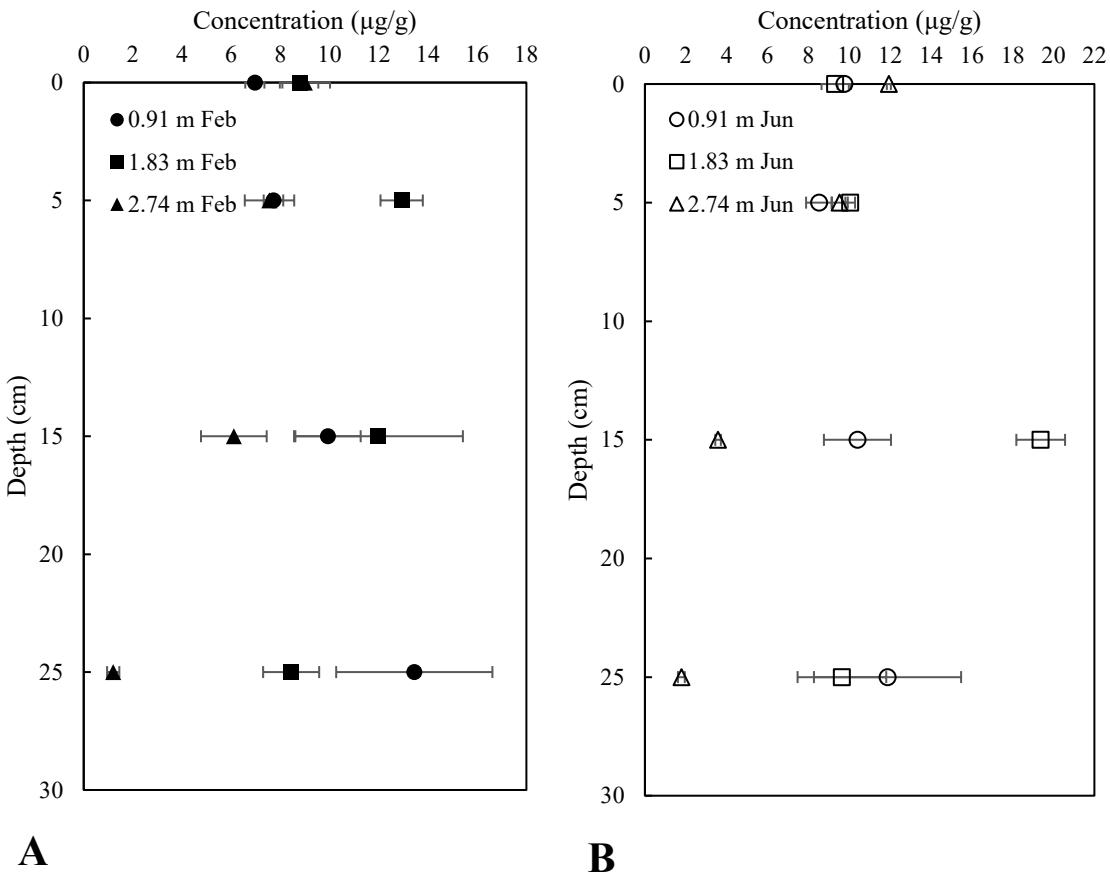

Figure A5. Total PAH concentrations of core samples. A: Total PAH concentration of core samples in February. B: Total PAH concentration of core samples in June (Error bars indicates the standard deviation of the samples)

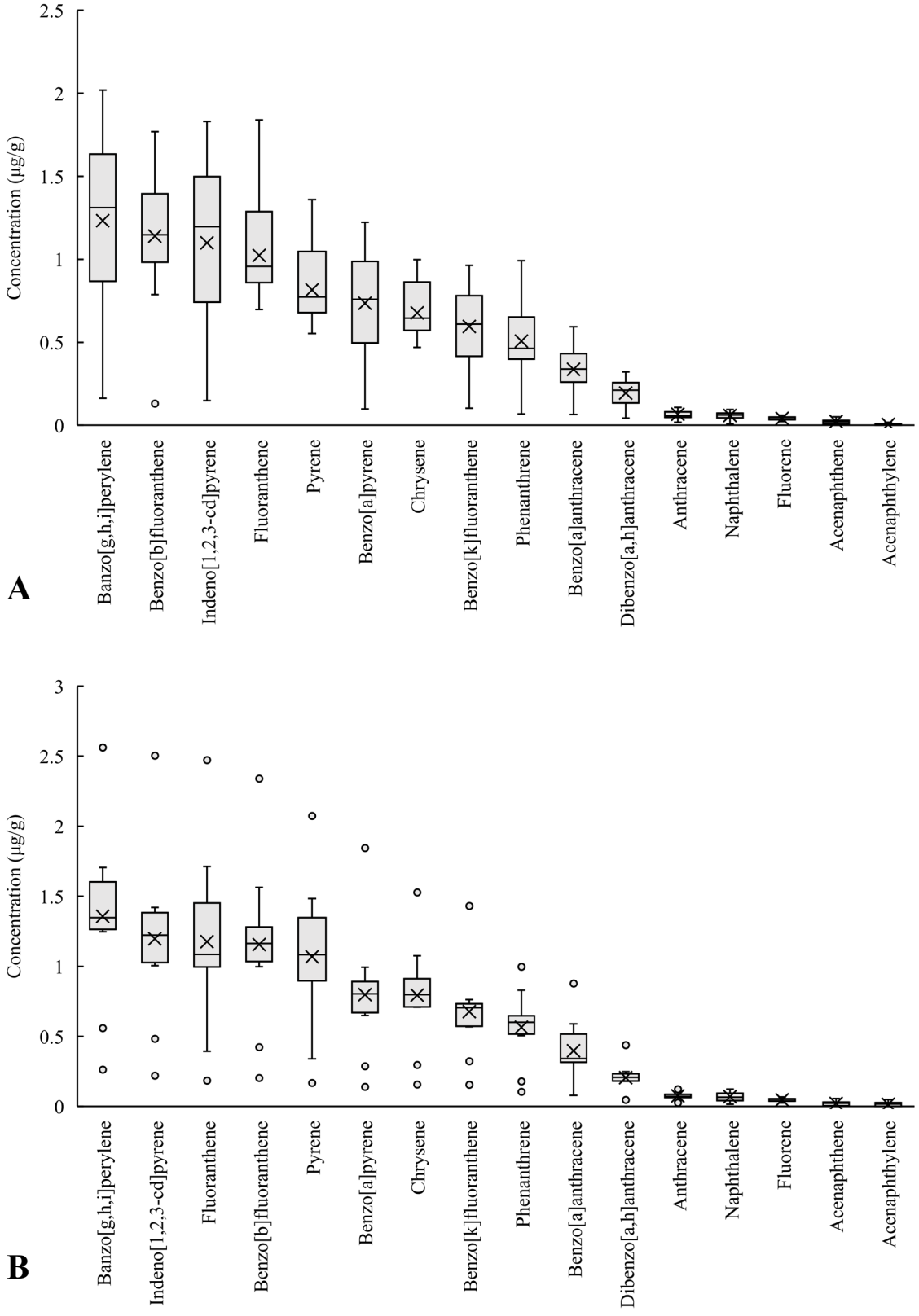
A
Concentration (µg/g)
2.5
2
1.5
1
0.5
0
Banzo[g,h,i]perylene
Benzo[b]fluoranthene
Indeno[1,2,3-cd]pyrene
Fluoranthene
Pyrene
Benzo[a]pyrene
Chrysene
Benzo[k]fluoranthene
Phenanthrene
Benzo[a]anthracene
Dibenzo[a,h]anthracene
Anthracene
Naphthalene
Fluorene
Acenaphthene
Acenaphthylene
B
Concentration (µg/g)
3
2.5
2
1.5
1
0.5
0
Banzo[g,h,i]perylene
Indeno[1,2,3-cd]pyrene
Fluoranthene
Benzo[b]fluoranthene
Pyrene
Benzo[a]pyrene
Chrysene
Benzo[k]fluoranthene
Phenanthrene
Benzo[a]anthracene
Dibenzo[a,h]anthracene
Anthracene
Naphthalene
Fluorene
Acenaphthene
Acenaphthylene

Figure A6. Individual PAH Concentrations in the surface and core samples at the bioretention cell (A: Concentrations of individual PAHs of samples in February. B: Concentrations of individual PAHs of samples in June. The upper and lower ends of the lines are the maximum and minimum values, the upper and lower ends of the boxes are quartiles, the middle segments of the boxes are the medians, the crosses represent the means, and the dots represent the outliers)

Table A4. Highest, lowest, and mean values of Total PAH and 16 PAHs, and compared with TECs and PECs (μg/g)

Compound name	Highest value	Lowest value	Mean	TEC[1]	PEC[1]	References
NAP	0.1235	0.0087	0.0639	0.1760	0.5610	MacDonald, et al. 2000
ACY	0.0497	<0.001	0.0107	0.0059	0.1280	CCME, 1998
ACE	0.0563	<0.001	0.0215	0.0067	0.0889	CCME, 1998
FLU	0.0670	0.0233	0.0442	0.0774	0.5360	MacDonald, et al. 2000
PHE	0.9960	0.0678	0.5362	0.2040	1.1700	MacDonald, et al. 2000
ANT	0.1440	0.0183	0.0708	0.0572	0.8450	MacDonald, et al. 2000
FLA	2.4717	0.1159	1.0998	0.4230	2.2300	MacDonald, et al. 2000
PYR	2.0726	0.1061	0.9410	0.1950	1.5200	MacDonald, et al. 2000
BaA	0.8763	0.0651	0.3679	0.1080	1.0500	MacDonald, et al. 2000
CHR	1.5273	0.1068	0.7364	0.1660	1.2900	MacDonald, et al. 2000
BbF	2.3402	0.1298	1.1477	0.2400	13.4000	Similar as below[2]
BkF	1.4302	0.1038	0.6356	0.2400	13.4000	Persaud et al. 1993
BaP	1.8448	0.0990	0.7665	0.1500	1.4500	MacDonald, et al. 2000
INP	2.5043	0.1480	1.1474	0.2000	3.2000	Persaud et al. 1993
DBA	0.4376	0.0439	0.1995	0.0330	1.3000	Persaud et al. 1993
BPY	2.5619	0.1633	1.2945	0.1700	3.2000	Persaud et al. 1993
Total PAH	19.3721	1.1996	9.0838	1.6100	22.8000	MacDonald, et al. 2000

[1]Values of TEC and PEC normalized by 1% total organic carbon (TOC) content, assumes that TOC of samples in bioretention cell and control samples were 1%.

[2]There are no guideline values for BbF, assumes that BbF have the same TEC and PEC value with BkF because of the similarity of their chemical structures.

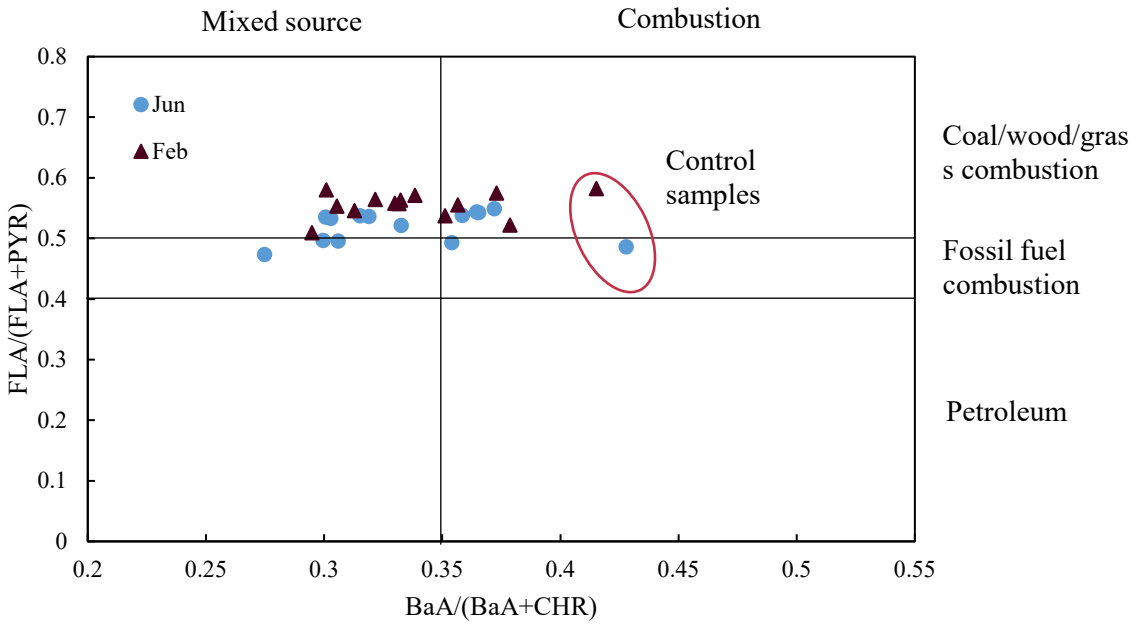

Figure A7. Diagnostic ratios of FLA/(FLA+PYR) against BaA/(BaA+CHR)

7.1 Future works

Some characteristics, such as total organic carbon, pH, and particle distribution of bioretention cell media will be measured to study their relationship with PAH concentration. More bacteria will be tested to be the positive control for PAH-RHD GP, PAH-RHD GN, and C23O primers. The gradient PCR will also be performed to positive cultures to find the optimal annealing temperatures for PAH-RHD GP, PAH-RHD GN, and C23O primers. After determining positive control and optimal annealing temperature for all primers, PCR will be conducted to all media samples and control samples, to do qualitative analysis of the presence of PAH degrading bacteria in the media. And qPCR will be used to do quantitative analysis of PAH degrading bacteria.

References

Al Ali, S., Debade, X., Chebbo, G., Béchet, B., and Bonhomme, C. 2017. Contribution of atmospheric dry deposition to stormwater loads for PAHs and trace metals in a small and highly trafficked urban road catchment. ***Environmental Science and Pollution Research***, 24(34): 26497-26512.

Bartlett, A., Rochfort, Q., Brown, L., and Marsalek, J. 2012. Causes of toxicity to Hyalella azteca in a stormwater management facility receiving highway runoff and snowmelt. Part I: Polycyclic aromatic hydrocarbons and metals. ***Science of the Total Environment***, 414: 227-237.

Brown, J. N., and Peake, B. M. 2006. Sources of heavy metals and polycyclic aromatic hydrocarbons in urban stormwater runoff. ***Science of the total environment***, 359(1-3): 145-155.

Cheng, C., Bi, C., Wang, D., Yu, Z., and Chen, Z. 2018. Atmospheric deposition of polycyclic aromatic hydrocarbons (PAHs) in Shanghai: the spatio-temporal variation and source identification. ***Frontiers of earth science***, 12(1): 63-71.

Crampon, M., Bureau, F., Akpa-Vinceslas, M., Bodilis, J., Machour, N., Le Derf, F., and Portet-Koltalo, F. 2014. Correlations between PAH bioavailability, degrading bacteria, and soil characteristics during PAH biodegradation in five diffusely contaminated dissimilar soils. ***Environmental Science and Pollution Research***, 21(13): 8133-8145.

David, N., Leatherbarrow, J. E., Yee, D., and McKee, L. J. 2014. Removal efficiencies of a bioretention system for trace metals, PCBs, PAHs, and dioxins in a semiarid environment. ***Journal of Environmental Engineering***, 141(6): 04014092.

DiBlasi, C. J., Li, H., Davis, A. P., and Ghosh, U. 2008. Removal and fate of polycyclic aromatic hydrocarbon pollutants in an urban stormwater bioretention facility. ***Environmental science & technology***, 43(2): 494-502.

Dickhut, R., Canuel, E., Gustafson, K., Liu, K., Arzayus, K., Walker, S., Edgecombe, G., Gaylor, M., and MacDonald, E. 2000. Automotive sources of carcinogenic polycyclic aromatic hydrocarbons associated with particulate matter in the Chesapeake Bay region. ***Environmental science & technology***, 34(21): 4635-4640.

El-Mufleh, A., Béchet, B., Grasset, L., Rodier, C., Gaudin, A., and Ruban, V. 2013. Distribution of PAH residues in humic and mineral fractions of sediments from stormwater infiltration basins. ***Journal of soils and sediments***, 13(3): 531-542.

EPA, U. 1993. Provisional guidance for quantitative risk assessment of polycyclic aromatic hydrocarbons. ***Development***: 1-28.

Esen, F., Cindoruk, S. S., and Tasdemir, Y. 2008. Bulk deposition of polycyclic aromatic hydrocarbons (PAHs) in an industrial site of Turkey. ***Environmental pollution***, 152(2): 461-467.

Galarneau, E. 2008. Source specificity and atmospheric processing of airborne PAHs:

implications for source apportionment. ***Atmospheric Environment***, 42(35): 8139-8149.

Gallagher, M. T., Snodgrass, J. W., Ownby, D. R., Brand, A. B., Casey, R. E., and Lev, S. 2011. Watershed-scale analysis of pollutant distributions in stormwater management ponds. ***Urban Ecosystems***, 14(3): 469-484.

Gauthier, P. T., Norwood, W. P., Prepas, E. E., and Pyle, G. G. 2014. Metal–PAH mixtures in the aquatic environment: a review of co-toxic mechanisms leading to more-than-additive outcomes. ***Aquatic toxicology***, 154: 253-269.

Haritash, A. K., and Kaushik, C. P. 2009. Biodegradation aspects of polycyclic aromatic hydrocarbons (PAHs): a review. ***Journal of hazardous materials***, 169(1-3): 1-15.

Herngren, L., Goonetilleke, A., Ayoko, G. A., and Mostert, M. M. 2010. Distribution of polycyclic aromatic hydrocarbons in urban stormwater in Queensland, Australia. ***Environmental pollution***, 158(9): 2848-2856.

Hong, E., Seagren, E. A., and Davis, A. P. 2006. Sustainable oil and grease removal from synthetic stormwater runoff using bench-scale bioretention studies. ***Water Environment Research***, 78(2): 141-155.

Hou, J., Bian, L., and Li, T. 2013. Characteristics and sources of polycyclic aromatic hydrocarbons in impervious surface run-off in an urban area in Shanghai, China. ***Journal of Zhejiang University SCIENCE A : Applied Physics & Engineering***, 14(10): 751-759.

Howitt, J. A., Mondon, J., Mitchell, B. D., Kidd, T., and Eshelman, B. 2014. Urban stormwater inputs to an adapted coastal wetland: role in water treatment and impacts on wetland biota. ***Science of the Total Environment***, 485: 534-544.

IARC. 2012. ***Review of Human Carcinogens: Chemical Agents and Related Occupations***: World health organization.

Istenič, D., Arias, C. A., Matamoros, V., Vollertsen, J., and Brix, H. 2011. Elimination and accumulation of polycyclic aromatic hydrocarbons in urban stormwater wet detention ponds. ***Water Science and Technology***, 64(4): 818-825.

Iwegbue, C. M., Iteku-Atata, E.-O. C., Odali, E. W., Egobueze, F. E., Tesi, G. O., Nwajei, G. E., and Martincigh, B. S. 2019. Distribution, sources and health risks of polycyclic aromatic hydrocarbons (PAHs) in household dusts from rural, semi-urban and urban areas in the Niger Delta, Nigeria. ***Exposure and Health***, 11(3): 209-225.

Jartun, M., Ottesen, R. T., Steinnes, E., and Volden, T. 2008. Runoff of particle bound pollutants from urban impervious surfaces studied by analysis of sediments from stormwater traps. ***Science of the Total Environment***, 396(2-3): 147-163.

Jiao, H., Bian, G., Chen, X., Wang, S., Zhuang, X., and Bai, Z. 2017. Distribution, sources, and potential risk of polycyclic aromatic hydrocarbons in soils from an industrial district in Shanxi, China. ***Environmental Science and Pollution Research***, 24(13): 12243-12260.

Kadri, T., Rouissi, T., Brar, S. K., Cledon, M., Sarma, S., and Verma, M. 2017. Biodegradation of polycyclic aromatic hydrocarbons (PAHs) by fungal enzymes: A review. ***Journal of environmental sciences***, 51: 52-74.

Kamalakkannan, R., Zettel, V., Goubatchev, A., Stead-Dexter, K., and Ward, N. I. 2004. Chemical (polycyclic aromatic hydrocarbon and heavy metal) levels in contaminated stormwater and sediments from a motorway dry detention pond drainage system. ***Journal of environmental monitoring***, 6(3): 175-181.

Kim, K.-H., Jahan, S. A., Kabir, E., and Brown, R. J. 2013. A review of airborne polycyclic aromatic hydrocarbons (PAHs) and their human health effects. ***Environment international***, 60: 71-80.

Kwon, H.-O., and Choi, S.-D. 2014. Polycyclic aromatic hydrocarbons (PAHs) in soils from a multi-industrial city, South Korea. ***Science of the Total Environment***, 470: 1494-1501.

Larsen, R. K., and Baker, J. E. 2003. Source apportionment of polycyclic aromatic hydrocarbons in the urban atmosphere: a comparison of three methods. ***Environmental Science & Technology***, 37(9): 1873-1881.

Lau, S.-L., Han, Y., Kang, J.-H., Kayhanian, M., and Stenstrom, M. K. 2009. Characteristics of highway stormwater runoff in Los Angeles: metals and polycyclic aromatic hydrocarbons. ***Water Environment Research***, 81(3): 308-318.

Lee, W.-J., Wang, Y.-F., Lin, T.-C., Chen, Y.-Y., Lin, W.-C., Ku, C.-C., and Cheng, J.-T. 1995. PAH characteristics in the ambient air of traffic-source. ***Science of the Total Environment***, 159(2-3): 185-200.

LeFevre, G. H., Novak, P. J., and Hozalski, R. M. 2011. Fate of naphthalene in laboratory-scale bioretention cells: implications for sustainable stormwater management. ***Environmental science & technology***, 46(2): 995-1002.

Li, H., and Davis, A. P. 2008. Heavy metal capture and accumulation in bioretention media. ***Environmental science & technology***, 42(14): 5247-5253.

Li, R., Zuo, Z., Chen, D., He, C., Chen, R., Chen, Y., and Wang, C. 2011. Inhibition by polycyclic aromatic hydrocarbons of ATPase activities in Sebastiscus marmoratus larvae: relationship with the development of early life stages. ***Marine environmental research***, 71(1): 86-90.

Lu, G.-N., Tao, X.-Q., Dang, Z., Yi, X.-Y., and Yang, C. 2008. Estimation of n-octanol/water partition coefficients of polycyclic aromatic hydrocarbons by quantum chemical descriptors. ***Open Chemistry***, 6(2): 310-318.

MacDonald, D. D., Ingersoll, C. G., and Berger, T. 2000. Development and evaluation of consensus-based sediment quality guidelines for freshwater ecosystems. ***Archives of environmental contamination and toxicology***, 39(1): 20-31.

Neira, C., Cossaboon, J., Mendoza, G., Hoh, E., and Levin, L. A. 2017. Occurrence and distribution of polycyclic aromatic hydrocarbons in surface sediments of San

Diego Bay marinas. ***Marine pollution bulletin***, 114(1): 466-479.

Nzila, A. 2018. Biodegradation of high-molecular-weight polycyclic aromatic hydrocarbons under anaerobic conditions: Overview of studies, proposed pathways and future perspectives. ***Environmental pollution***, 239: 788-802.

Parnis, J. M., Mackay, D., and Harner, T. 2015. Temperature dependence of Henry's law constants and KOA for simple and heteroatom-substituted PAHs by COSMO-RS. ***Atmospheric Environment***, 110: 27-35.

Pies, C., Hoffmann, B., Petrowsky, J., Yang, Y., Ternes, T. A., and Hofmann, T. 2008. Characterization and source identification of polycyclic aromatic hydrocarbons (PAHs) in river bank soils. ***Chemosphere***, 72(10): 1594-1601.

Pyrene, N. R. C. C. o., and Analogues, S. 1983. ***Polycyclic aromatic hydrocarbons: evaluation of sources and effects***: National Academies Press.

Ribeiro, C. O., Vollaire, Y., Sanchez-Chardi, A., and Roche, H. 2005. Bioaccumulation and the effects of organochlorine pesticides, PAH and heavy metals in the Eel (Anguilla anguilla) at the Camargue Nature Reserve, France. ***Aquatic Toxicology***, 74(1): 53-69.

Sałata, A., and Dąbek, L. 2017. ***Sediments from stormwater drainage system as sorbents of organic and inorganic pollutants***. Paper presented at the E3S Web of Conferences.

Siddens, L. K., Larkin, A., Krueger, S. K., Bradfield, C. A., Waters, K. M., Tilton, S. C.,

Pereira, C. B., Löhr, C. V., Arlt, V. M., and Phillips, D. H. 2012. Polycyclic aromatic hydrocarbons as skin carcinogens: comparison of benzo [a] pyrene, dibenzo [def, p] chrysene and three environmental mixtures in the FVB/N mouse. ***Toxicology and applied pharmacology***, 264(3): 377-386.

Sikkema, J., de Bont, J. A., and Poolman, B. 1994. Interactions of cyclic hydrocarbons with biological membranes. ***Journal of Biological Chemistry***, 269(11): 8022-8028.

Syed, K., Doddapaneni, H., Subramanian, V., Lam, Y. W., and Yadav, J. S. 2010. Genome-to-function characterization of novel fungal P450 monooxygenases oxidizing polycyclic aromatic hydrocarbons (PAHs). ***Biochemical and biophysical research communications***, 399(4): 492-497.

Thomas, F., Lorgeoux, C., Faure, P., Billet, D., and Cébron, A. 2016. Isolation and substrate screening of polycyclic aromatic hydrocarbon degrading bacteria from soil with long history of contamination. ***International Biodeterioration & Biodegradation***, 107: 1-9.

Wang, X.-T., Miao, Y., Zhang, Y., Li, Y.-C., Wu, M.-H., and Yu, G. 2013. Polycyclic aromatic hydrocarbons (PAHs) in urban soils of the megacity Shanghai: occurrence, source apportionment and potential human health risk. ***Science of the Total Environment***, 447: 80-89.

Watts, A. W., Ballestero, T. P., Roseen, R. M., and Houle, J. P. 2010. Polycyclic aromatic

hydrocarbons in stormwater runoff from sealcoated pavements. ***Environmental science & technology***, 44(23): 8849-8854.

Weinstein, J. E., Crawford, K. D., Garner, T. R., and Flemming, A. J. 2010. Screening-level ecological and human health risk assessment of polycyclic aromatic hydrocarbons in stormwater detention pond sediments of Coastal South Carolina, USA. ***Journal of Hazardous Materials***, 178(1-3): 906-916.

Wongwongsee, W., Chareanpat, P., and Pinyakong, O. 2013. Abilities and genes for PAH biodegradation of bacteria isolated from mangrove sediments from the central of Thailand. ***Marine pollution bulletin***, 74(1): 95-104.

Yang, B., Zhou, L., Xue, N., Li, F., Li, Y., Vogt, R. D., Cong, X., Yan, Y., and Liu, B. 2013. Source apportionment of polycyclic aromatic hydrocarbons in soils of Huanghuai Plain, China: comparison of three receptor models. ***Science of the Total Environment***, 443: 31-39.

Yunker, M. B., Macdonald, R. W., Vingarzan, R., Mitchell, R. H., Goyette, D., and Sylvestre, S. 2002. PAHs in the Fraser River basin: a critical appraisal of PAH ratios as indicators of PAH source and composition. ***Organic geochemistry***, 33(4): 489-515.

Yunker, M. B., Perreault, A., and Lowe, C. J. 2012. Source apportionment of elevated PAH concentrations in sediments near deep marine outfalls in Esquimalt and Victoria, BC, Canada: is coal from an 1891 shipwreck the source? ***Organic***

Geochemistry, 46: 12-37.

Zgheib, S., Moilleron, R., Saad, M., and Chebbo, G. 2011. Partition of pollution between dissolved and particulate phases: what about emerging substances in urban stormwater catchments? ***Water Research***, 45(2): 913-925.

Chapter 2

Thesis Conclusion

Thesis conclusion

The study evaluated the effectiveness of a bioretention cell for the removal of PAHs in stormwater. This was done by comparing control samples collected near the bioretention cell with the bioretention cell media samples. The results showed that the bioretention cell contained 9.70 times higher levels of total PAH than the control samples. It was found that PAHs accumulated in the media might have a negative impact on the environment by being ingested by surrounding organisms and bioaccumulating. A comparison between samples collected in this study with samples from the same location collected in 2008, it was found that PAHs accumulated in the media 5 cm below the surface. This finding provides new information that is relevant for the management of bioretention cells. PAHs tend to accumulate in the media due to their relatively low bioavailability. If allowed to accumulate, PAHs will eventually break through the media, overload the media adsorption capacity and enter the aquatic environment thus causing contamination of nearby waterways. Therefore, it is important to determine and implement proper maintenance frequency and routines of the bioretention cell. The maintenance could be replacing contaminated media with clean media or to further biotransformation. Evaluation of the sources of PAHs found those detected in the bioretention cell mainly originated from petroleum source and fossil fuel combustion source. This corresponds to the location of the bioretention cell, where it collects stormwater from parking lots and roads. This result reveals the importance of using

stormwater management facilities alongside roads to prevent PAH pollution. The study of the PAH carcinogenicity in the media revealed that benzo[a]pyrene (BaP) contributed the most, although it did not have the highest concentration of the individual PAHs, which illustrates the importance of BaP as a carcinogen. This result can help to improve the management of stormwater bioretention cells by for example evaluating the effect of stormwater treatment. Here the BaP concentration can be used as an important indicator. Therefore, when designing stormwater management facilities along roadways, the BaP treatment capacity should be considered.

To conduct a more in-depth study of the accumulation of PAHs in bioretention cell, more research is still needed. First, the relationship between characteristics of media and PAHs needs to be studied by determining the distribution of PAHs associated with media particles of different sizes as well as, the relationship between the TOC of the media and the concentration of PAHs. Also, in this study the presence of PAH transforming bacteria was performed but was cut short due to the University Shutdown in March 2020. Therefore, this part of the study will continue by applying molecular biology tools to evaluate the potential for in situ PAH degradation in the bioretention media. If the bacteria are present, conditions for enhancement of their activity will be determined.

Based on the current conclusions, it is not clear whether biodegradation of PAHs has occurred in the media of the bioretention cell in this study, but the accumulation of PAHs in the media indicates that the degradation rates of PAHs should be less than their

accumulation rates. As a result, it is necessary to strengthen the biodegradation of PAH in media.

The half-lives of PAHs in soil are related to their molecular weights. The half-life of phenanthrene is 16 to 126 days, while the half-life of benzo[a]pyrene is 229 to 2100 days (Shuttleworth and Cerniglia, 1995). Biostimulation and bioaugmentation have been successfully used to enhance the biodegradation of PAH in soil and solid waste. Nagalakshmi (2019) removed 99% PAHs from soil by biostimulation in 56 days. To improved biodegradation of PAHs, Lladó (2013) biostimulated industrial polluted soil by adding lignocellulosic substrate, soybean oil and Manganese ions, and 76% PAHs were removed in 60 days. Sun (2012) combined biostimulation and bioaugmentation to treat PAHs-contaminated soil. 43.9% and 55.0% of total PAHs and HMW-PAH were degraded in 175 days, respectively. Since the environment of bioretention cell media is similar to soil, biostimulation and bioaugmentation can also be used to degrade PAHs in the bioretention cell media. The bioremediation methods used in the bioretention cell will depend on the microbial community in the media. If there are enough PAH degrading bacteria in the media, biostimulation can be used. If there are insufficient PAH degrading bacteria in the media, bioaugmentation should be used to add PAH degrading bacteria to the media. Biostimulation and bioaugmentation can also be used in combination to to enhance the biodegradability of the PAHs in the media. This will improve the life span and sustainability of bioretention cell and limit the requirements for management.

References

Haleyur, N., Shahsavari, E., Jain, S. S., Koshlaf, E., Ravindran, V. B., Morrison, P. D., Osborn, A. M., and Ball, A. S. 2019. Influence of bioaugmentation and biostimulation on PAH degradation in aged contaminated soils: Response and dynamics of the bacterial community. ***Journal of environmental management***, 238: 49-58.

Lladó, S., Covino, S., Solanas, A., Viñas, M., Petruccioli, M., and D'annibale, A. 2013. Comparative assessment of bioremediation approaches to highly recalcitrant PAH degradation in a real industrial polluted soil. ***Journal of hazardous materials***, 248: 407-414.

Shuttleworth, K. L., and Cerniglia, E. 1995. Environmental aspects of PAH biodegradation. ***Applied biochemistry and biotechnology***, 54(1-3): 291-302.

Sun, G.-D., Xu, Y., Jin, J.-H., Zhong, Z.-P., Liu, Y., Luo, M., and Liu, Z.-P. 2012. Pilot scale ex-situ bioremediation of heavily PAHs-contaminated soil by indigenous microorganisms and bioaugmentation by a PAHs-degrading and bioemulsifier-producing strain. ***Journal of hazardous materials***, 233: 72-78.